

Thermal Analysis of Repository Codisposal Waste Packages Containing Melt-Dilute Aluminum Spent Nuclear Fuel

by

S. Y. Lee

Westinghouse Savannah River Company

Savannah River Site

Aiken, South Carolina 29808

DOE Contract No. DE-AC09-96SR18500

This paper was prepared in connection with work done under the above contract number with the U. S. Department of Energy. By acceptance of this paper, the publisher and/or recipient acknowledges the U. S. Government's right to retain a nonexclusive, royalty-free license in and to any copyright covering this paper, along with the right to reproduce and to authorize others to reproduce all or part of the copyrighted paper.

Thermal Analysis of Repository Codisposal Waste Packages Containing Melt-Dilute Aluminum Spent Nuclear Fuel

Si Young Lee

UNCLASSIFIED
DOES NOT
UNCLASSIFIED
INCLUDE
ADC &
Refueling
Office
Date: 5/19/99

William Smith Mgr. ENRS

Westinghouse Savannah River Company
Savannah River Site
Aiken, SC 29808



SAVANNAH RIVER SITE

DISCLAIMER

This report was prepared as an account of work sponsored by an agency of the United States Government. Neither the United States Government nor any agency thereof, nor any of their employees, makes any warranty, express or implied, or assumes any legal liability or responsibility for the accuracy, completeness, or usefulness of any information, apparatus, product, or process disclosed, or represents that its use would not infringe privately owned rights. Reference herein to any specific commercial product, process, or service by trade name, trademark, manufacturer, or otherwise does not necessarily constitute or imply its endorsement, recommendation, or favoring by the United States Government or any agency thereof. The views and opinions of authors expressed herein do not necessarily state or reflect those of the United States Government or any agency thereof.

This report has been reproduced directly from the best available copy.

Available to DOE and DOE contractors from the Office of Scientific and Technical Information, P.O. Box 62, Oak Ridge, TN 37831; prices available from (615) 576-8401.

Available to the public from the National Technical Information Service, U.S. Department of Commerce, 5285 Port Royal Road, Springfield, VA 22161.

DISCLAIMER

Portions of this document may be illegible in electronic image products. Images are produced from the best available original document.

WSRC-TR-98-00299

KEYWORDS:

Thermal Analysis
Spent Nuclear Fuel
Co-Disposal Waste Package
Decay Heat Source
Melt-Dilute Co-Disposal
RETENTION - Permanent

Thermal Analysis of Repository Codisposal Waste Packages Containing Melt-Dilute Aluminum Spent Nuclear Fuel

SAVANNAH RIVER TECHNOLOGY CENTER

Si Young Lee

Publication Date: April, 1999

Westinghouse Savannah River Company
Savannah River Site
Aiken, SC 29808



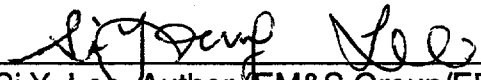
SAVANNAH RIVER SITE

Prepared for the U.S. Department of Energy under Contract No. DE-AC09-96SR18500

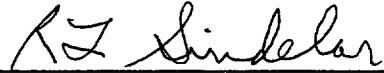
(This Page Intentionally Left Blank)

DOCUMENT: WSRC-TR-98-00299
TITLE: Thermal Analysis of Repository Codisposal Waste Packages Containing Melt-Dilute Aluminum Spent Nuclear Fuel (U)
TASK: SRT-MTS-97-2030

APPROVALS



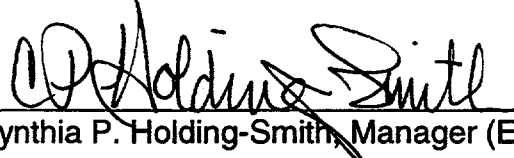
Si Y. Lee, Author (EM&S Group/EDS/SRTC) Date: 4-19-99



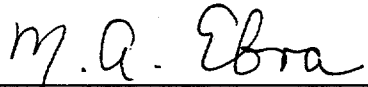
Robert L. Sindelar, SNF Task Leader (MTS/SRTC) Date: 4-19-99



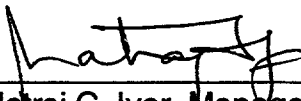
Poh-Sang Lam, Technical Reviewer (MTS/SRTC) Date: 4-19-99



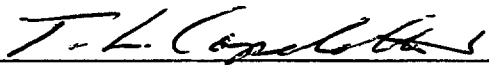
Cynthia P. Holding-Smith, Manager (EM&S Group/SRTC) Date: 5/7/99



Martha A. Ebra, Manager (EDS/SRTC) Date: 5/16/99



Natraj C. Iyer, Manager (SNF Programs /SRTC) Date: 5/4/99



Tami L. Capeletti, Manager (MTS /SRTC) Date: 5/18/99



William F. Swift, Customer (SFS Engineering) Date: 5/3/99

(This Page Intentionally Left Blank)

Table of Contents

Abstract	1
1 Introduction	2
2 Acceptance Criteria	4
3 Analysis Approach for Codisposal Waste Package	7
3.1 General Governing Equations and Solution Method	7
3.2 Conduction Model	16
3.3 Baseline Model	16
4 Modeling Assumptions and Design Parameters	18
5 Results and Discussions	26
6 Conclusions	53
7 Recommendations	54
8 References	55

(This Page Intentionally Left Blank)

List of Figures

Figure 1.	Horizontal emplacement of codisposal waste package in the center of drift repository.....	6
Figure 2.	Simplified diagram for thermal analysis approach methodology of codisposal waste package containing the melt-dilute AI-SNF form.....	8
Figure 3.	Non-dimensional decay heat sources for melt-dilute SNF and HWGL regions as a function of storage time. Non-dimensional decay source is defined as the ratio of transient decay heat to initial decay heat.	9
Figure 4.	Typical temperature and buoyancy-driven velocity profiles due to physical energy transport mechanism in an enclosed WP geometry.	11
Figure 5.	Thermal Modeling of codisposal SNF waste package in a geological repository.....	14
Figure 6.	Non-uniform mesh grids of computational domain on the x-y plane for the present model.....	15
Figure 7.	Mesh cells associated with the interface between the neighboring cells of two different material regions	18
Figure 8.	Wall heat transfer characteristics from the horizontal curved surface of the WP into the ambient air region of a drift tunnel.....	20
Figure 9.	Qualitative temperature distributions predicted by the three models under the present codisposal WP configuration.....	29
Figure 10.	Radial temperature distribution of He-cooled 100% volume melt-dilute codisposal WP for various storage times based on the baseline model.....	35
Figure 11.	Temperature contour plot for He-cooled 100% volume melt-dilute codisposal WP based on the baseline model at 0 years of storage time.	36
Figure 12.	Radial temperature distribution of Air-cooled 100% volume melt-dilute codisposal WP for various storage times based on the baseline model.....	37
Figure 13.	Temperature contour plot for air-cooled 100% volume melt-dilute codisposal WP based on the baseline model at 0 years of storage time.	38
Figure 14.	Comparison of maximum temperatures for He-cooled and air-cooled 100% volume melt-dilute codisposal WP's for various storage times based on the baseline model.....	39
Figure 15.	Non-dimensional radial temperature distributions for He-cooled melt-dilute and direct AI-SNF codisposal WP's for 50 and 100 volume percentages of SNF based on the baseline model at 0 years of storage time.	40
Figure 16.	Comparison of maximum temperatures for He-cooled melt-dilute codisposal WP's for various ingot volume percentages of the SNF canister at 0 years of storage time based on the baseline model.....	41
Figure 17.	Non-dimensional radial temperature distribution for He-cooled melt-dilute codisposal WP for various volume percentages of SNF based on the baseline model at 0 years of storage time.	42
Figure 18.	Temperature contour plot for He-cooled 90% volume melt-dilute codisposal WP based on the baseline model at 0 years of storage time.	43
Figure 19.	Comparison of maximum temperatures for He-cooled 100% and 90% volume melt-dilute codisposal WP's for various geological ambient temperatures based on the baseline model.	44

Figure 20.	Comparison of radial temperatures for He-cooled 100% and 90% volume melt-dilute codisposal WP's for 0 year's initial reference storage time based on the baseline model (ambient temperature = 150 °C).	45
Figure 21.	Maximum temperatures of air-cooled and helium-cooled 100 vol% melt-dilute codisposal waste packages with bounding SNF decay heat loads for various geological ambient temperatures.	46
Figure 22.	Comparison of centerline temperature distributions based on the baseline model and the conduction model for helium-cooled 100 vol% melt-dilute codisposal WP with 100% Cs decay heat source.	47
Figure 23.	Comparison of centerline temperature distributions based on the baseline model, the conduction model, and the detailed model for helium-cooled 50 vol% melt-dilute codisposal WP with 100% Cs decay heat source at 0 years of storage time.	48
Figure 24.	Comparison of radial temperature distributions along the line A-A' based on the baseline model and the detailed model for helium-cooled direct codisposal WP with with 100% Cs decay heat source at 0 years of storage time.	49
Figure 25.	Velocity vector plot of back-filled gas motion due to natural convection based on the detailed model for helium-cooled 50 vol% melt-dilute codisposal WP with 100% Cs decay heat source at 0 years of storage time.	50
Figure 26.	Temperature contour plot over the entire computational domain based on the detailed model for helium-cooled 50 vol% melt-dilute codisposal WP with 100% Cs decay heat source at 0 years of storage time.	51
Figure 27.	Back-filled gas flow pattern due to natural convective cooling within codisposal waste package.	52

List of Tables

Table 1.	Status of thermal performance analysis for repository codisposal waste packages containing DOE Al-SNF canister.	3
Table 2.	Decay heat source in SNF canister and HWGL regions for codisposal WP filled to 100 % of SNF volume with melt-dilute ingot containing 100% Cs.	21
Table 3.	Decay heat source in SNF canister and HWGL regions for codisposal WP filled to 90 % of SNF volume with melt-dilute ingot containing 100% Cs.	22
Table 4.	Decay heat source in SNF canister and HWGL regions for codisposal WP filled to 75 % of SNF volume with melt-dilute ingot containing 100% Cs.	23
Table 5.	Decay heat source in SNF canister and HWGL regions for codisposal WP filled to 50 % of SNF volume with melt-dilute ingot containing 100% Cs.	24
Table 6.	Reference design conditions for the present thermal analysis.	25
Table 7.	Thermal and radiation properties of the codisposal WP components containing melt-dilute Al-SNF form used for the present analysis (Ref. 8).	27
Table 8.	Typical levels of radiative cooling contributions to the thermal performance of the He-cooled codisposal WP containing 100 vol.% and 50 vol.% melt-dilute SNF forms.	29
Table 9.	Level of radiative cooling contribution to the thermal performance of the He-cooled codisposal WP containing 100 vol.% melt-dilute SNF form.	29
Table 10.	Comparison of peak temperatures for the codisposal WP with 100 vol.% SNF canister containing 100% Cs in melt-dilute alloy ingot based on the baseline model for various storage times (ambient temperature = 100 °C).	30
Table 11.	Comparison of peak temperatures for the He-cooled codisposal WP with various volume percentages of SNF canister containing 20% Cs and 100%	

	Cs in melt-dilute alloy ingot based on the baseline model for various storage times (ambient temperature = 100 °C).....	31
Table 12.	Comparison of peak and wall temperatures for the He-cooled and air-cooled codisposal packages with 50 and 100 volume percentages of SNF canister containing 100% Cs in melt-dilute alloy ingot based on the baseline model at 0 years of storage times under the reference design conditions of Table 6.	31
Table 13.	Comparison of peak and wall temperatures for the He-cooled codisposal WP with various volume percentages of SNF canister containing 100% Cs in melt-dilute alloy ingot based on the baseline model at 0 years of storage times under the reference design conditions of Table 6.....	32
Table 14.	Comparison of peak temperatures for the He-cooled codisposal WP with two different volume percentages of SNF canister containing 100% Cs in melt-dilute alloy ingot based on the baseline model for various ambient temperatures at 0 years of storage time.	33
Table 15.	Comparison of peak temperatures for the He-cooled and air-cooled codisposal WP's with 100 volume percentage of SNF canister containing 100% Cs in melt-dilute alloy ingot based on the baseline model for various ambient temperatures at 0 years of storage time.....	33

(This Page Intentionally Left Blank)

Abstract

The engineering viability of disposal of aluminum-clad, aluminum-based spent nuclear fuel (Al-SNF) in a geologic repository requires a thermal analysis to provide the temperature history of the waste form. Calculated temperatures are used to demonstrate compliance with criteria for waste acceptance into the Mined Geologic Disposal System and as input to assess the chemical and physical behavior of the waste form within the waste package.

A thermal analysis methodology has been developed to calculate peak temperatures and temperature profiles of Al-SNF in the DOE spent nuclear fuel canister within a codisposal waste package. A two-dimensional baseline model with conduction and radiation coupled heat transport was developed to evaluate the thermal performance for both the direct and the melt-dilute Al-SNF forms in a codisposal Waste Package (WP) over the range of possible heat loads and boundary conditions. In addition, a conduction model and a detailed model which includes convection were developed to identify the dominant cooling mechanism under the present WP configuration, to investigate physical cooling mechanism in detail, and to estimate the conservatism imbedded in the baseline model. The approach methodology and all the detailed results for the direct and the melt-dilute Al-SNF forms in the codisposal WP containing the SNF canister, which was filled with 75% or 90% of the SNF canister volume, were documented in Reference [1]. The decay heat loads for the melt-dilute Al-SNF canister were based on the assumption that 80% of Cs isotope was volatilized or released during a melting and dilution process of the SNF assemblies into the DOE SNF canister.

The present report documents the additional results using the previous methodology [1] for the He-cooled codisposal WP containing 100%, 90%, 75%, and 50% of the SNF canister volume filled with melt-dilute ingot. The report also includes the results of thermal performance analysis for the air-cooled codisposal WP containing 100% and 90% of the SNF canister volume. The previous conduction model and the detailed model are also used to estimate the conservatism imbedded in the baseline model under various fuel volume percentages of the melt-dilute Al-SNF forms. For the present analysis, decay heat source of the SNF is estimated using the conservative assumption that cesium (Cs) isotopes are not released during the melting process, which results in the same decay heat as the direct disposal option with upper bounding source.

The results of the baseline model showed that the melt-dilute disposition configurations with helium-filled and air-filled Waste Packages (WP's) satisfied the present acceptance criteria for the WP design in terms of the peak temperature criterion, $T_{\max} \leq 350$ °C, under reference boundary conditions. A period of 10 years' cooling time for the decay heat loads of the SNF and the High-level Waste Glass Log (HWGL) regions was used as one of the reference design conditions.

Many of the reference conditions are not confirmed yet. For example, waste package and DOE SNF canister materials and dimensions and the thermal history of the repository will change as the final designs are developed. When the key information affecting the thermal performance of the waste forms is confirmed, the present baseline model will be used to analyze the final design configuration.

1 Introduction

A thermal analysis is performed to calculate peak temperatures and profiles of the codisposal waste package (WP) under reference design conditions as a function of storage time. The leading codisposal WP design proposes that a central DOE spent nuclear fuel (SNF) canister be surrounded by five Defense Waste Process Facility (DWPF) glass log canisters, that is, High-level Waste Glass Logs (HWGL's), and placed into a WP in the Mined Geologic Disposal System (MGDS). The waste package is cylindrical with a diameter of about 6 ft. A DOE SNF canister having about 17 inch diameter and about 10 ft length is placed along the central horizontal axis of the waste package. The five HWGL's, each with a 2 ft diameter and 10 ft length, will be located around the peripheral region of the DOE SNF canister within the WP container. The codisposal WP will be laid down horizontally in a drift repository as shown in Fig. 1.

There are two waste form options for AI-SNF disposition using the codisposal WP design configuration. They are:

- the direct AI-SNF form, and the
- melt-dilute AI-SNF form.

For the direct form option, a total of up to 64 standard-sized Material Test Reactor (MTR) type AI-SNF fuel assemblies, some with highly-enriched U, are to be packed in a DOE SNF canister. For the melt-dilute form option, a number of AI-SNF assemblies are melted and diluted to be emplaced in the central DOE SNF stainless steel canister, which result in a SNF canister containing uranium-aluminum alloy ingots.

For the present analysis, a SNF canister is assumed to be filled to 100% of the canister volume with a uranium-aluminum alloy ingot, which results in the melt-dilution process. In addition, thermal analyses for 90%, 75%, and 50% SNF of the canister volume are conducted to examine the WP performance with respect to different SNF volume percentages. The decay heat source of the SNF is assumed to contain 100% Cs without any volatilization of cesium isotopes during melt-dilution process. The present report includes the thermal performance analysis of the codisposal WP containing the SNF canister filling various percentages of the canister volume with the 100% Cs melt-dilute alloy ingot. It is important to examine the WP performance with respect to different SNF volume percentages since there is possibility to contain air bubbles inside the metal ingot or rough ingot surface during the melting process. The composition of an ingot will have the eutectic composition of the binary alloy (13.2 wt. % uranium, 86.8 wt. % aluminum) with less than and equal to 20% enriched uranium-235. The transient decay heat loads used in the present analysis included: i) the melt-dilute form for the case where all the krypton and 100% of the cesium assumed to be remained in alloy ingot; and ii) the HWGL. Detailed discussions for the decay heat loads are provided in Ref. [1].

Thermal performance analysis of the codisposal WP for licensing will be performed for the specific design conditions and thermal history of a geological repository. This information is not available at this time. Therefore, reference design conditions are assumed to perform the analyses. The assumed reference conditions are shown in Section 4 (see Table 6). In addition, sensitivity analyses for key design parameters of the codisposal WP are performed over a range of boundary conditions.

The objective of the present study is to perform the thermal analyses of codisposal storage configurations containing the 100, 90, 75, and 50 vol.% melt-dilute ingot of the SNF canister volume. The same methodology as provided by Ref. [1] is used to estimate the SNF, HWGL, and WP temperatures in a geological repository for various boundary conditions. Table 1 shows the status of thermal performance analysis for the codisposal WP containing DOE AI-SNF canister.

Table 1. Status of thermal performance analysis for repository codisposal waste packages containing DOE AI-SNF canister.

SNF Disposal Options	Back-filled Gas	Decay Heat Loads	Loading Volume of SNF Canister	Documentation of Analysis Results
Direct Disposal	Helium or Air	Upper bounding	64 fuel assemblies	Done (Ref. 1)
		Nominal	64 fuel assemblies	Done (Ref. 1)
Melt-Dilute Disposal	Helium or Air	20 % Cs (80% Cs removed during the process)	75 vol. %	Done (Ref. 1)
			90 vol. %	Done (Ref. 1)
		100% Cs	100 vol. %	Present analysis
	90 vol. %		Present analysis	
	Helium	100% Cs	75 vol. %	Present analysis
			50 vol. %	Present analysis

This report addresses thermal performance internal to the codisposal WP since thermal analysis modeling of hydro-geological media including the geological drift tunnel region is beyond the scope of the present work. The present model boundary line is shown in Fig. 1. Three thermal models have been developed to assess the thermal performance of the codisposal WP design using intact prototypic geometry created under the body-fitted coordinate system in the computational fluid dynamics (CFD) preprocessing environment. The first model considers conduction only. The second model is the baseline model including the conduction and radiation cooling mechanisms under various combinations of decay heat source terms and codisposal WP design parameters. The present baseline analysis uses the baseline model based on a parametric approach to evaluate thermal performance for each WP design option since the baseline model is the most efficient one among them in terms of computational time and reasonable accuracy. The third model is the detailed model considering the convection and radiation as well as conduction cooling processes to estimate the conservatism of the baseline model for a typical design condition and to understand the physical cooling mechanism in full detail for the present codisposal WP design. The detailed model results are also included in the present report although it is expected to have the results similar to those of the previous report [Ref. 1]. The CFX code [3] has been used as a tool to model and simulate the thermal performance for the codisposal WP's in a drift geological tunnel repository. It had been previously used to simulate and benchmark the test data for the interim dry SNF storage canister with reasonable accuracy [4].

The thermal analysis results will be used to demonstrate compliance with the waste acceptance criteria for the MGDS and as input to assess the chemical and physical behavior of the Al-SNF forms within the WP.

2 Acceptance Criteria

Criteria for acceptance of SNF and high-level waste forms into the federal repository or MGDS are being compiled by the U. S. Department of Energy, Office of Civilian Radioactive Waste Management (OCRWM) as part of the preparation for submission of the system for licensing by the Nuclear Regulatory Commission. The development of the repository acceptance criteria is understood to be an ongoing process. The present draft criteria are contained in Reference 5, the MGDS Draft Disposability Interface Specification. In this recent draft, the criteria are referred to as "disposability standards."

The approach in the Alternative Technology Program is to show conformance with the disposability standards [6]. Two standards from Reference 5 can be addressed using the results from the heat source development work [2] and thermal analysis work in this report. The demonstration of conformance would need to be updated as both the disposability standards and the design of the MGDS waste package and DOE SNF canister evolve.

Disposability Standard 2.4.20 - Limits on Total Thermal Output for Disposable Canisters specifies that "no disposable single-element SNF canister shall have a thermal output in excess of 1500 watts at the time of shipment to the MGDS. Multi-element canister thermal outputs are addressed in Disposability Standard 2.4.21." Tables 2 through 5 in this report show that the highest total thermal output of the various loading configurations of Al SNF forms in the DOE canister is 1158 watts, well-within the 1500

watt standard. The time of zero years in the tables corresponds to a time of ten years cool down following reactor operation with the assembly.

Disposability Standard 2.4.21 – Limits on Disposable Multi-Element Canister Thermal Design specifies that “SNF cladding for assemblies placed in disposable canisters shall not exceed 350 °C. This shall be shown through calculation to be achievable over 1000 years. This calculation shall include the following inputs and assumptions.

- Decay heat assumed in the calculation shall be calculated using decay-heat generation curves appropriate for the specific SNF in the canister.
- Temperatures at the canister surface should be assumed to be as follows, with “Year Zero” defined as the time the canister leaves the waste-custodian site.

<u>Year</u>	<u>Temperature</u>
0-1	150 °C
1-5	175 °C
5-50	190 °C
> 50	200 °C

The detailed thermal modeling and analysis in this report for the assumed reference conditions show that the temperature criterion is met. Figures 10 and 24 are the WP temperature profile results for using the upper bound heat sources for the direct and melt-dilute forms, respectively, with a helium gas backfill in both the DOE SNF and the WP. The AI SNF form maximum temperature is below 350 °C even with the canister temperature above 200 °C at time zero. It should be noted that the present calculations provide information that shows that temperatures are below the temperature limit. As previously stated, this information will support the performance assessment of the AI SNF forms under repository conditions including interactions with packaging materials.

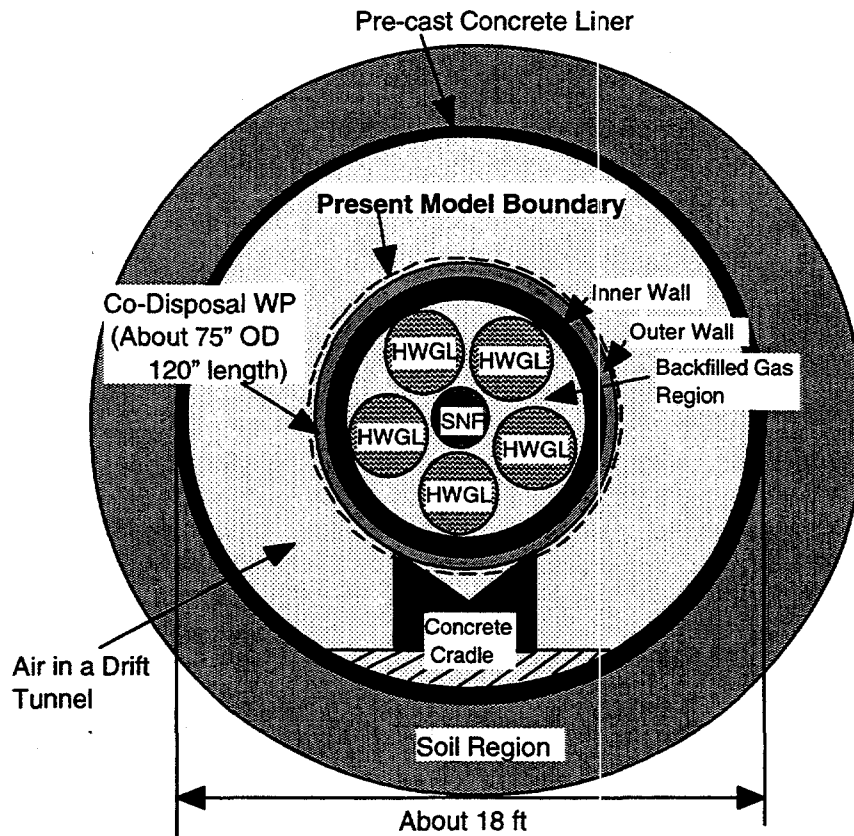


Figure 1. Horizontal emplacement of codisposal waste package in the center of drift repository.

3 Analysis Approach for Codisposal Waste Package

Thermal performance analysis for the codisposal WP design for one of the two Al-SNF form options, namely, the melt-dilute form, is performed as a function of storage time for various boundary conditions by using a parametric analysis approach. The initial storage time, "Year 0", is defined as the time the canister leaves the site and is put into the WP container and emplaced in the repository. For the present analysis, the initial time for the SNF and the HWGL is assumed to be 10 years' cooling time after fuel discharge from the reactor and after the production of high-level waste glass log. The WP temperatures are then computed for selected times during the first 2000 years after emplacement in the repository. A quasi-steady state temperature distribution is assumed for each selected time since the package transient temperatures will reach equilibrium in a few days. The present modeling boundary is shown in Fig. 1. For a typical reference design condition such as helium-cooled, intact codisposal WP, the physical cooling mechanism has been also investigated to understand how decay heat energy is transported through the WP to the geological environment. Specifically, how the waste package temperature affects the buoyancy-driven natural circulation inside the WP, and what is the most dominant mode of thermal energy transport for the present codisposal WP configuration have been investigated [1]. This information may be important to assess corrosion degradation of the WP and to determine the movement of moisture outside the WP boundary. The approach methodology for the present thermal analysis is shown in Fig. 2.

3.1 General Governing Equations and Solution Method

The codisposal WP contains five HWGL's and one central SNF canister. The codisposal canister is horizontal at the center of a geological drift tunnel as schematically shown in Fig. 1. The HWGL and SNF regions have different decay heat sources, and the SNF canister is surrounded by five HWGL canisters. The WP will be filled with air or helium, possibly in combination with other filler material such as neutron poisons, depending on the design. Solid regions of the SNF and HWGL canisters have time-dependent heat sources. The present thermal analysis uses well-defined heat source terms for the SNF and HWGL regions [Ref. 1]. Thermal and material properties for structural materials of the WP and the melt-dilute ingot are also defined [Refs. 1, 7, and 8]. Typical transient decay heat curves for the HWGL and the melt-dilute DOE SNF forms are shown in Fig. 3. The non-dimensional decay heat shown in the figure is the ratio of decay heat at storage time t to initial decay heat load. Initial decay heat powers are 8.58 W per assembly for the melt-dilute SNF option with 100% Cs (5.63 W per SNF assembly in case of 20% Cs) and 472.3 W per HWGL, respectively. The present analysis is using the upper bounding decay heat source with 100% Cs. Table 2 in Section 4 shows transient decay powers and their corresponding volumetric power densities as a function of storage time.

The heat generated by the nuclear decay process will be transferred by back-filled gas medium and eventually will be transported to the geological medium through the physical mechanisms of conduction, convection, and radiation heat transport processes. In this situation the decay heat energy of the SNF and HWGL regions is transported from one point to another in a solid medium only through conduction mechanism. The heat transfer at the solid-fluid interface boundary is computed using thermal conductivity

of the gas and fluid temperature gradient at the solid wall boundary. The fluid temperature gradient at the wall is dependent on the gas flow field driven by the density gradient at the wall boundary layer since the temperature gradient is dependent on the rate at which the gas fluid convects the heat away. Thus energy transport is coupled to the momentum transport through the wall interface of the solid and fluid regions.

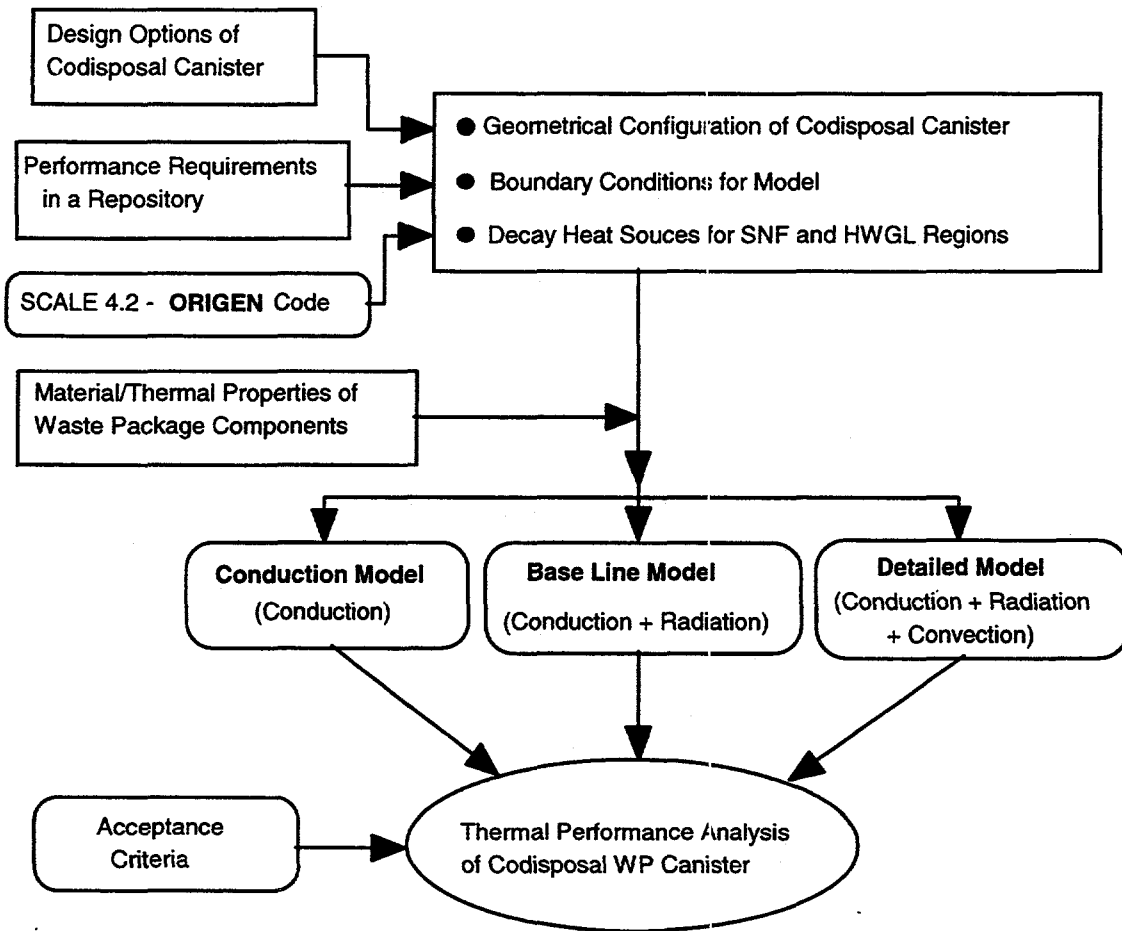


Figure 2. Simplified diagram for thermal analysis approach methodology of codisposal waste package containing the melt-dilute Al-SNF form

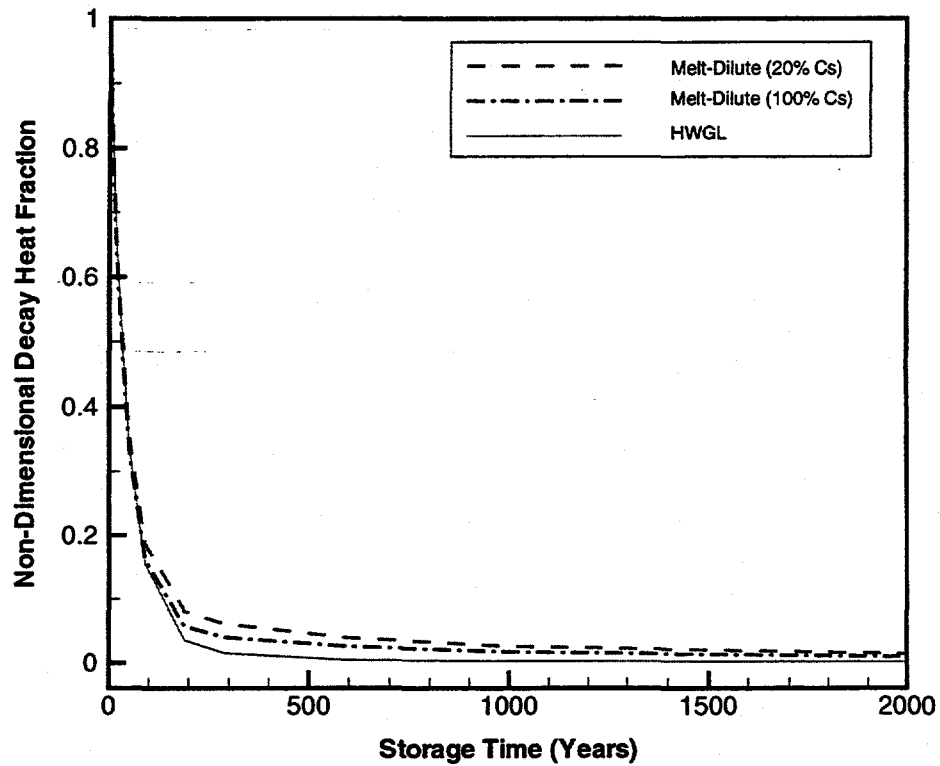


Figure 3. Non-dimensional decay heat sources for melt-dilute SNF and HWGL regions as a function of storage time. Non-dimensional decay source is defined as the ratio of transient decay heat to initial decay heat.

In contrast to the mechanisms of the conduction and convection, where energy transport through a material medium is involved, heat may also be transferred by the propagation of electromagnetic wave through the gas or vacuum in case of high temperature environment. This electromagnetic radiation is emitted at the surface of a solid body which has been thermally excited; and when it strikes another body, part may be reflected, part may be transmitted, and part may be absorbed. If the incident radiation is thermal radiation with the proper wavelength, the absorbed radiation will appear as heat within the absorbing body. Heat due to the radiation mechanism may pass from one body to another without the need of a medium of transport between them. Like the present situation, there may be a separating medium, such as helium or air, which is unaffected by this passage of energy. There will be a continuous interchange of energy between two radiating bodies, with a net exchange of energy from the hotter to the colder. The basic governing equations of thermal energy transport must be coupled with those of fluid motion and electromagnetic radiation of body surface in order to describe, mathematically, the process of energy transfer. Therefore, the detailed model considered heat transfer mechanisms driven by convection and radiation as well as conduction within an enclosed codisposal WP.

Typical flow and temperature profiles within the codisposal WP containing direct AI-SNF form under actual process of energy transport mechanism including a buoyancy-driven natural convection due to the fluid temperature gradient were illustrated in the previous reports [1, 4]. Figure 4 also illustrates actual process of energy transport mechanism including a buoyancy-driven natural convection caused by the fluid temperature gradient. Temperature decreases rapidly due to the convective and radiative cooling effects within a boundary layer region, as shown in the previous results [1]. The boundary layer flow is a buoyancy-induced motion resulting from body forces acting on density gradients which, in turn, arise from temperature gradients in the fluid. It is virtually impossible to observe pure heat conduction in a gas medium because as soon as a temperature difference is imposed on a fluid, natural convection currents will occur as a result of density differences. The gravitational body force is oriented in the negative y-direction for the present analysis.

The governing equations for the present two-dimensional analysis under the Cartesian coordinate system are shown below.

For the mass continuity,

$$\frac{\partial \rho}{\partial t} + \frac{\partial(\rho u)}{\partial x} + \frac{\partial(\rho v)}{\partial y} = 0 \quad (1)$$

In eq. (1) ρ is the density of the medium and u and v are the local velocities in the x and y directions, respectively.

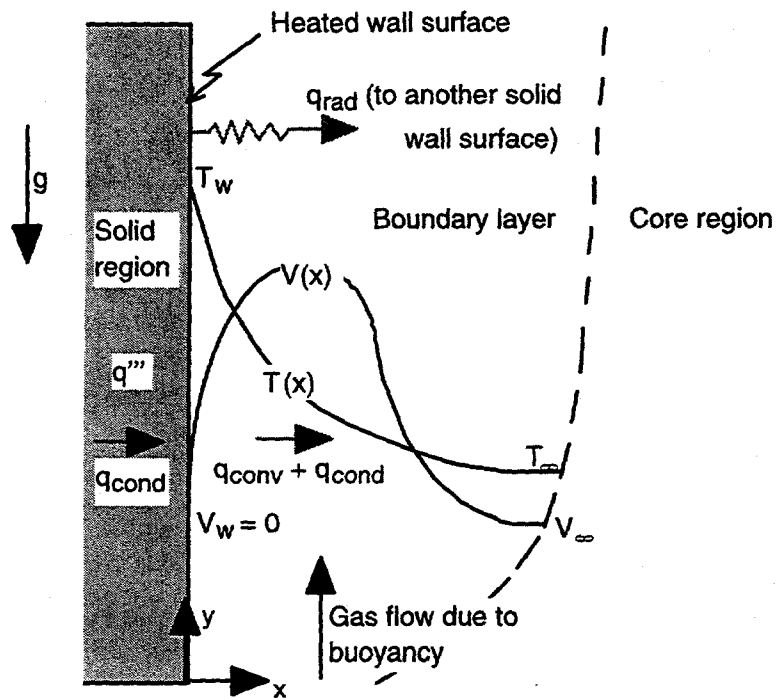


Figure 4. Typical temperature and buoyancy-driven velocity profiles due to physical energy transport mechanism in an enclosed WP geometry.

For the momentum equation in tensor notation,

$$\rho \left(\frac{\partial u_i}{\partial t} + u_j \frac{\partial u_i}{\partial x_j} \right) = \frac{\partial \sigma_{ij}}{\partial x_j} + X_i \quad (2)$$

where the variables with the subscript, i (or j) = 1, or 2, correspond to those of the x -, or y -direction, respectively. σ_{ij} is the stress tensor and X_i the body force term.

$$\sigma_{ij} = -P\delta_{ij} + \mu \left(\frac{\partial u_i}{\partial x_j} + \frac{\partial u_j}{\partial x_i} \right)$$

$$\delta_{ij} = \begin{cases} 1 & \text{for } i = j \\ 0 & \text{for } i \neq j \end{cases}$$

$X_i = 0$ for the present model and P = fluid pressure.

For a general energy balance equation on a control volume of the waste package,

$$\rho \frac{Dh}{Dt} - \frac{\partial}{\partial x} \left\{ k \frac{\partial T}{\partial x} \right\} - \frac{\partial}{\partial y} \left\{ k \frac{\partial T}{\partial y} \right\} + \frac{\partial}{\partial x} \{ q_{rad,x} \} + \frac{\partial}{\partial y} \{ q_{rad,y} \} - \beta T \frac{DP}{Dt} - \Phi - q''' = 0 \quad (3)$$

where Φ is viscous dissipation term, h thermodynamic enthalpy, $q_{rad, x}$, $q_{rad, y}$ radiative heat fluxes in the x - and y -directions, and q''' heat generation source term. The viscous dissipation term is not included in the present model.

From eq. (3), energy terms within a control volume of a fluid medium in the waste package includes convection ($\bar{v} \cdot \nabla T$), conduction ($k \nabla T$), radiation heat transfer (q_r), internal heat sources (q'''), compression work of back-filled gas ($\beta T(DP/Dt)$), and energy storage due to transients ($\rho \partial h / \partial t = \rho C_p \partial T / \partial t$). Storage of radiant energy within the control volume is generally negligible; hence no modification of the usual transient terms will be considered as a result of the radiation field. Radiation pressure is negligible relative to the fluid pressure and hence does not contribute to the compression work term. Assuming that probability of emission of a given photon wavelength (λ) for any surface in an enclosure obeys Kirchoff's law and surface is diffuse-gray, $\epsilon(\lambda) = \alpha(\lambda) = \epsilon$, where emissivity (ϵ) is independent of wave length. The intervening back-filled gas medium is assumed to have no absorption or emission. ϵ is always less than 1.0 since real surfaces emit and absorb less radiant energy than a black body. Radiative heat flux in eq. (3) then becomes

$$q_{rad, m} = \alpha(q)_{black\ body} = \alpha \sigma T^4 = \epsilon \sigma T^4 \quad (4)$$

where $m = x$ or y .

In eq. (4) α and ϵ are absorption and emission coefficients of wall surface, and σ is Stefan-Boltzman's constant ($5.670 \times 10^{-8} \text{ W/m}^2\text{K}^4$). Under the present SNF storage conditions, the energy storage due to transients, viscous dissipation, and gas compression work terms are negligible relative to the main heat transfer mechanisms such as conduction, convection, and radiation.

For the detailed modeling analysis, the Boussinesq approximation was used for the gravitational term in the momentum equation to include the buoyancy-induced natural convection. It is a two-part approximation: It neglects all variable property effects in the governing equations and it approximates the density difference term with a simplified equation of state, that is, the gravity term in the y -direction, $X_2 = -\rho g$, in eq. (2) is replaced by the following relation:

$$\rho g = \rho_{\infty} \{1 - \beta(T - T_{\infty})\} g \quad (5)$$

where β is thermal expansion coefficient, and ρ_{∞} is the density at $T = T_{\infty}$.

Natural convective flow regimes for the helium-cooled and the air-cooled WP designs may be estimated based on the non-dimensional quantity, Grashof number (Gr_L), which is the parameter describing the ratio of buoyancy to viscous forces. The Grashof number performs much the same function for natural convection flow as the Reynolds (Re) number does for forced convection. Under normal conditions one may expect that the laminar-to-turbulent transition will take place at about $Gr_L \approx 10^9$.

For a typical helium-cooled WP design,

$$Gr_L = \frac{g\beta L^3 (T_w - T_\infty)}{\nu^2} \quad (6)$$

$$\approx 1.40 \times 10^7 < 1.0 \times 10^9 \text{ (laminar flow)}$$

where L = characteristic length parameter (=1.7545 m),

β = thermal expansion coefficient (= $2.00 \times 10^{-3} \text{ K}^{-1}$),

T_w = wall temperature,

T_∞ = ambient temperature,

ν = kinematic viscosity (= $2.91 \times 10^{-4} \text{ m}^2/\text{sec}$).

For air-cooled WP design, Grashof number (Gr_L) is

$$Gr_L \approx 7.35 \times 10^8$$

where $\beta = 2.00 \times 10^{-3} \text{ K}^{-1}$,

$$\nu = 3.80 \times 10^{-5} \text{ m}^2/\text{sec}.$$

This corresponds to the near-transition flow according to the literature information (Ref. 9). For the present analysis, natural convection regime within the waste package is assumed to be laminar.

These governing equations are applied to the two-dimensional computation domain depending on the physical model for the thermal performance analysis of the codisposal WP. A 1/2 sector model of the codisposal WP was used as a computational domain for a better computational efficiency by imposing symmetrical boundary conditions on the diagonal centerline of the WP cross-sectional plane. Fig. 5 presents the present 1/2 sector model including the symmetry plane and six different material zones.

The two-dimensional geometry file was created using the multi-block preprocessor of the CFX code under the body-fitted coordinate system, which allows the treatment of non-orthogonal geometry. For the present analysis, an optimum grid of 9822 cells has been established from the grid sensitivity analysis under SGI workstation environment. The WP canister model consists of 195 element blocks and 6 different material zones on the x-y computational plane. Non-uniform two-dimensional meshes of the computational domain are presented in Fig. 6. Adequacy of grid fineness for the present computational domain was illustrated in Ref. [1]. Numerical solution technique to solve the governing equations was also described in Ref. [1].

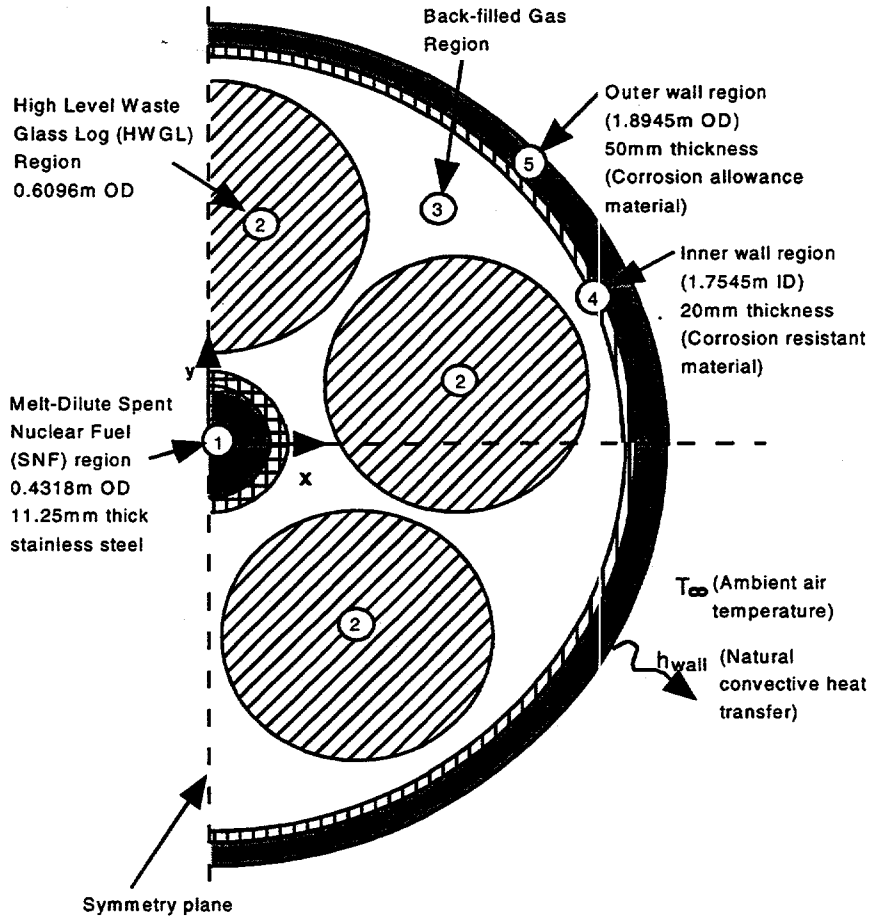


Figure 5. Thermal Modeling of codisposal SNF waste package in a geological repository.

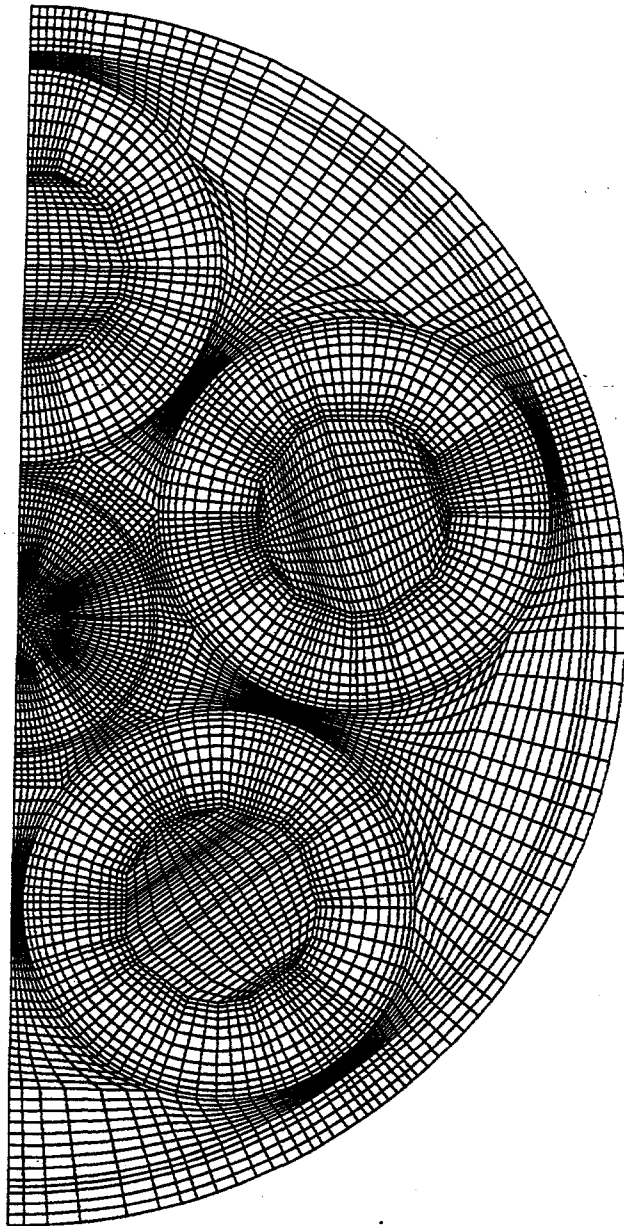


Figure 6. Non-uniform mesh grids of computational domain on the x-y plane for the present model

3.2 Conduction Model

The mathematical equation governing conductive cooling in the WP medium can be obtained from the energy balance equation (3) neglecting the contributions of convection and radiation terms. In this model, convective cooling due to buoyancy-driven gas circulation and radiative cooling effect are neglected, which leads to extremely conservative estimation for thermal performance of the codisposal design. Energy balance equation corresponding to the conduction model for the material region having thermal conductivity k becomes

$$\rho C_p \left(\frac{\partial T}{\partial t} \right) = \nabla \cdot (k \nabla T) + q''' \quad (7)$$

The primary objectives for performing the thermal analyses using a conduction model, a conduction-radiation coupled model (baseline model), and a conduction, radiation, and convection model (detailed model) are:

- (a) to find out what the upper bounding estimation is in terms of thermal performance of the present codisposal WP and
- (b) to investigate what the most dominant cooling mechanism is for the present codisposal WP design configuration among the three potential cooling modes, conduction, radiation, and convection, using the other two model results. A 1/2 sector geometry model of the codisposal WP was used for a better computational efficiency by imposing symmetrical boundary conditions on the centerline of the package as shown in Fig. 5.

3.3 Baseline Model

The baseline model neglects natural convective cooling mechanism driven by back-filled gas buoyancy due to temperature gradient in a back-filled gas medium of the codisposal WP compared to conduction and thermal radiative heat transfer mechanisms. However, the detailed model considers convective cooling effect along with conduction and radiation to quantify the conservatism imbedded in the baseline model.

The previous analysis results [1] show that thermal energy transport due to conduction and radiation cooling effects plays key role in the assessment of thermal performance of the codisposal WP. Thus, only the energy balance on a control volume of the WP is considered for the baseline modeling analysis. Mass and momentum transports due to natural convection become zero assuming that gas medium within the WP enclosure is frozen. In this situation energy balance equation, eq. (3), can be rewritten in a vector form in terms of heat flux and transient temperature for a control volume of the computational domain with volumetric decay heat source (q''').

$$\rho C_p \left(\frac{\partial T}{\partial t} \right) = \nabla \cdot (\bar{q}_{cond} - \bar{q}_{rad}) + q''' \quad (8)$$

As shown in eq. (8), the net inflow of radiant energy per unit volume can be written as the negative of the divergence of a radiant heat flux vector \bar{q}_{rad} . In eq. (8) T denotes temperature at time (t) for a medium of material density (ρ), specific heat (C_p), and

volumetric heat source (q'''). q_{cond} and q_{rad} are conductive and radiative heat fluxes, respectively.

For the thermal performance analysis of the melt-dilute codisposal WP in a geological repository, a quasi-steady state temperature distribution is assumed for each selected time since the WP transient temperatures will reach equilibrium in a few days. For steady state condition with no heat source in a transparent and frozen gas medium, energy balance given by eq. (8) becomes

$$\begin{aligned} & \text{(Heat Conducted into Surface } i, q_{\text{cond},i}) \\ & = \text{(Radiant Heat lost from Surface } i, q_{\text{rad},i}) \end{aligned} \quad (9)$$

When convection term is not included for the baseline model, the heat conducted into a wall surface is balanced by the radiant heat lost from the wall surface as shown in eq. (9). For solid wall surface i , conductive heat flux $q_{\text{cond},i}$ in a two-dimensional computational domain becomes

$$q_{\text{cond},i} = k \left(\frac{\partial T}{\partial x} + \frac{\partial T}{\partial y} \right)_{\text{surface},i} \quad (10)$$

In eq. (10) k is thermal conductivity.

From the present model, non-uniform conductivity can arise from the nonhomogeneous material such as a composite annulus layer as shown in Fig. 7. It is considered that the control volume surrounding the grid point P is filled with a material of uniform conductivity k_P , and the one around E with a material of conductivity k_E . The notations are described in Fig. 7. For the composite layer between points P and E , a steady analysis without source in the x -direction leads to

$$q_{x,i} = \left(\frac{1}{\frac{(\Delta x)_{i-}}{k_P} + \frac{(\Delta x)_{i+}}{k_E}} \right) (T_P - T_E)_{x,i} = \left(\frac{k_i}{(\Delta x)_i} \right) (T_P - T_E)_{x,i} \quad (11)$$

When interpolation factor, $f_{x,i} = \left(\frac{(\Delta x)_{i+}}{(\Delta x)_i} \right)$, is introduced, eq. (11) becomes

$$q_{x,i} = \left(\frac{k_i}{(\Delta x)_i} \right) (T_P - T_E)_{x,i} = \left(\frac{k_P k_E}{(1-f_{x,i})k_E + f_{x,i}k_P} \right) \frac{(T_P - T_E)_{x,i}}{(\Delta x)_i} \quad (12)$$

Equation (12) shows that k_i , thermal conductivity at the interface i , is the harmonic average of thermal conductivities, k_P and k_E , of the two different neighboring materials, material A and material B.

Total emissive radiation heat flux of a wall surface i at temperature T within an enclosure become

$$q_{\text{rad},i} = \varepsilon_{\text{surface},i} q_{\text{black body},i} = \sigma (\varepsilon T^4)_{\text{surface},i} \quad (13)$$

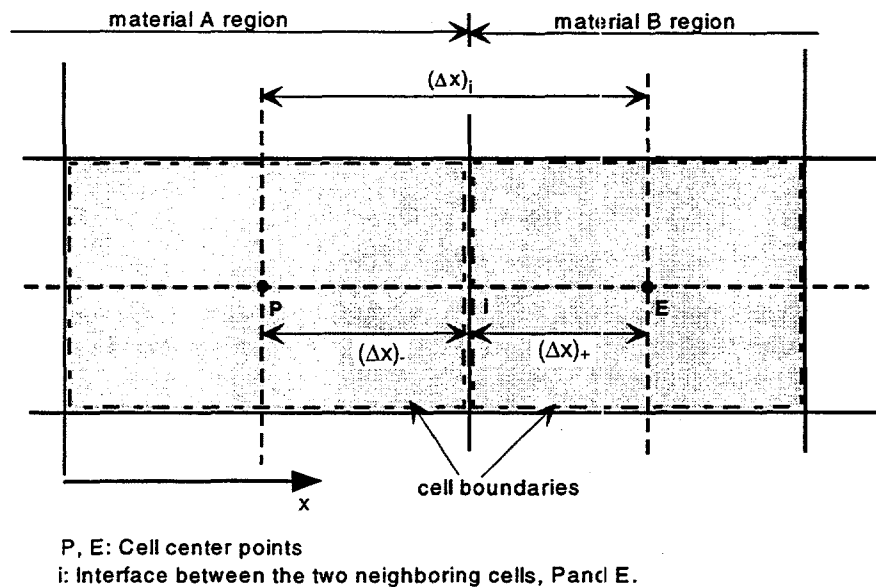


Figure 7. Mesh cells associated with the interface between the neighboring cells of two different material regions

In eqs. (12) and (13), the information on thermal conductivities (k_p and k_e) and wall surface emissivity ($\epsilon_{\text{surface}}$) of the WP components is required to find out the temperature distributions of the SNF and HWGL packages within the codisposal WP. The material and radiation properties for the present analysis are provided in Table 5. For the present baseline analysis, a two-dimensional, steady state, conduction-radiation coupled model was developed using uniformly-distributed heat generation sources within the HWGL region and SNF canister to predict the codisposal package thermal performance in a geological repository. In the previous analysis [1], buoyancy-induced natural convection term was considered for the detailed model to simulate thermal performance of the waste package and to quantify the conservatism of the conduction-radiation model. The model used a 1/2 sector geometry model of the codisposal WP for a better computational efficiency by imposing symmetrical boundary conditions on the centerline of the package as shown in Fig. 4. The baseline model will be used for the sensitivity runs with respect to the reference conditions. The reference conditions are shown in Table 1. The detailed numerical solution technique for the present governing equations, the adequacy of the grid fineness for the solution accuracy, and the residual error checking to demonstrate the adequacy of the grid fineness were documented in Ref. [1].

Finally, the analysis results will be provided to the degradation model of the waste package for the structural integrity analysis.

4 Modeling Assumptions and Design Parameters

The present analyses are made for the thermal performance of the codisposal WP containing melt-dilute uranium-aluminum alloy ingot of DOE Al-SNF based on the alternative SNF disposal technology. The computational modeling domain is shown in

Fig. 5. Figure 6 presents two-dimensional computational meshes used for the present analysis. A quasi-steady state temperature distribution was assumed for a selected storage time since the waste package transient temperatures will reach equilibrium in a few days. The package was assumed to be laid down horizontally at the center of the geological repository drift tunnel as shown in Fig. 1. The geological ambient temperature around the package wall circumference was assumed to be uniform.

A typical natural convective heat transfer coefficient (h) of $1.5 \text{ W/m}^2\text{ }^\circ\text{C}$ was used as an external wall boundary condition for the present analysis. The present value of the heat transfer coefficient can be justified on the following basis:

For horizontally-oriented geometrical configuration illustrated by Fig. 7, heat transfer coefficient (h) for natural convective cooling under laminar flow regime ($Ra = Gr_L Pr < 10^9$) is given in terms of non-dimensional numbers empirically.

$$Nu_L = \frac{hD}{k} = C(Gr_L Pr)^m \quad \text{for } Gr_L Pr > 10^4 \quad (12)$$

where C and m are the coefficients determined by the literature data. D is outer diameter of the WP, and Pr is the Prandtl number defined by $(\mu C_p / k)$.

$$Gr_L = \frac{g\beta\rho^2(T_{wall} - T_\infty)L^3}{\mu^2} \quad (13)$$

T_{wall} and T_∞ in eq. (13) are WP wall and ambient air temperatures, respectively. β is thermal expansion coefficient, that is,

$$\begin{aligned} \beta &= -\frac{1}{\rho} \left(\frac{\partial \rho}{\partial T} \right)_P \\ &= \frac{1}{T} \quad (\text{for ideal gas assumption}) \end{aligned} \quad (14)$$

For the present geometrical configuration shown in Fig. 8, $C=0.525$ and $m=0.25$ are given by Chapman (1974) using the experimental data [9]. From eq. (12), heat transfer coefficient (h) is about $1.5 \text{ W/m}^2\text{ }^\circ\text{C}$ corresponding to $Nu_L \approx 97$ conservatively under the present conditions. Theoretical approach was also taken to compute conservative natural convective heat transfer rate by using boundary layer theory in the previous work [10].

Natural convection due to internal gas movement inside the waste package is neglected in the baseline model. However, it was considered in the detailed model to investigate internal cooling mechanism of the codisposal WP containing aluminum-clad DOE SNF in detail since the baseline model can not capture the physical cooling mechanism due to natural circulation within the WP container [1]. Effective thermal conductivity for the melt-dilute ingot of the SNF canister was used as the value of Al-13.2wt% uranium metal alloy [1, 8]. Heat load for each of the SNF and HWGL regions was provided to the present models (see eq. (3), (7), or (8)) as volumetric heat input source (q''') by assuming that decay heat generation for each region is uniformly distributed. The bounding decay heat load was estimated by assuming that no cesium isotopes were removed during the melting process. The volumetric heat load for the melt-dilute SNF ingot filled with 100% of the SNF canister volume is presented as a function of storage

time in Table 2. The volumetric decay heat source for melt-dilute ingot filled with 90%, 75%, or 50% of the SNF canister volume is shown in Table 3 to Table 5.

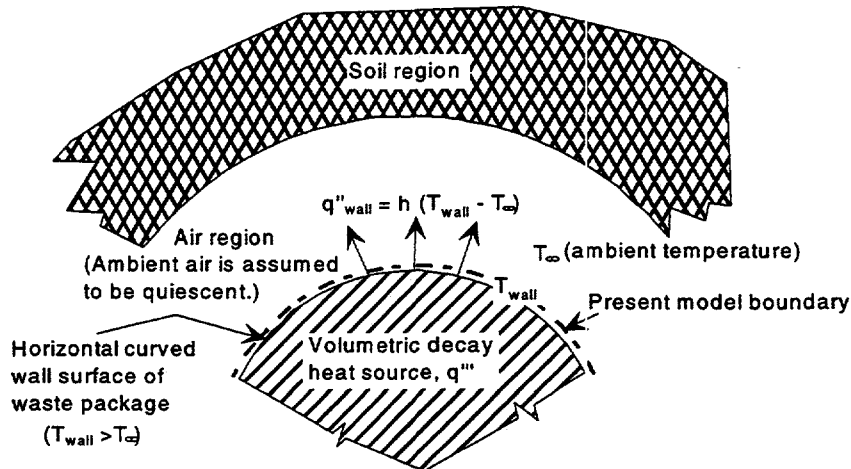


Figure 8. Wall heat transfer characteristics from the horizontal curved surface of the WP into the ambient air region of a drift tunnel.

The main design parameters involved in the thermal performance of the codisposal WP containing melt-dilute Al-SNF form are:

- Different combinations of back-filled gases in the SNF canister and the WP container (e.g., air-air, helium-helium)
- Various sets of combinations of two heat sources (bounding or nominal SNF and HWGL decay heat sources): Bounding decay heat sources for the SNF and HWGL are used for the present analysis since nominal SNF source was considered for the sensitivity analysis in the previous work [1].
- Initial reference storage time related to the spent fuel cooling time before the emplacement of aluminum-clad DOE SNF assemblies into the WP container: 10 years' cooling time is used as the reference storage time "0" year for the present analysis. The previous analysis showed the results for various cooling times [1].
- Internal structure materials of codisposal canister: The present analysis is assumed that SNF and HWGL canisters inside the WP remain intact.
- Various different volume fractions of SNF inside the canister
- Repository temperature history since emplacement of WP
- Waste package location in a repository drift tunnel (center or corner of a drift tunnel): The present analysis is assumed that WP is located at the center of a drift tunnel repository.

The thermal performance analysis for the codisposal WP requires known values for the design parameters listed above to study design options for a codisposal WP. Some of them are not available at this time. For the present work, initial reference time is assumed to be 10 years' cooling time since the discharge from reactor and production of HWGL. It is also assumed to have no solid conduction paths among the SNF and HWGL canisters such that HWGL canisters, SNF canister, and codisposal canister inner wall do not touch each other since final geometrical configuration is neither confirmed nor available yet. Thus, reference design conditions are used to perform the baseline analysis of the melt-dilute codisposal WP as shown in Table 6. Sensitivity analyses for some of the main design parameters are performed with respect to the reference conditions.

Table 2. Decay heat source in SNF canister and HWGL regions for codisposal WP filled to 100 % of SNF volume with melt-dilute ingot containing 100% Cs.

Storage Time (yrs)	Assembly Power (W/assembly)	Power per HWGL (W)	Total Power for SNF Can. (W)	Volumetric SNF Power (W/m ³)	Volumetric HWGL Power (W/m ³)
0	8.58	472.3	1158.30	2888.24	530.91
10	6.53	375.99	881.55	2198.16	422.65
20	5.243	301.35	707.81	1764.92	338.75
50	2.83	159.5	382.05	952.65	179.29
90	1.382	73.1	186.57	465.22	82.17
190	0.487	16.81	65.75	163.94	18.90
290	0.3442	7.09	46.47	115.87	7.97
590	0.2218	1.98	29.94	74.66	2.23
990	0.1468	1.14	19.82	49.42	1.28
1990	0.0794	0.72	10.72	26.73	0.81
2990	0.063	0.62	8.51	21.21	0.70
5990	0.0505	0.52	6.82	17.00	0.58
9990	0.041	0.43	5.54	13.80	0.48
19990	0.0265	0.3	3.58	8.92	0.34
49990	0.0103	0.16	1.39	3.47	0.18
99990	0.0034	0.11	0.46	1.14	0.12

Table 3. Decay heat source in SNF canister and HWGL regions for codisposal WP filled to 90 % of SNF volume with melt-dilute ingot containing 100% Cs.

Storage Time (yrs)	Assembly Power (W/assembly)	Power per HWGL (W)	Total Power for SNF Can. (W)	Volumetric SNF Power (W/m ³)	Volumetric HWGL Power (W/m ³)
0	8.58	472.3	1038.18	2876.35	530.91
10	6.53	375.99	790.13	2189.11	422.65
20	5.243	301.35	634.40	1757.66	338.75
50	2.83	159.5	342.43	948.73	179.29
90	1.382	73.1	167.22	463.30	82.17
190	0.487	16.81	58.93	163.26	18.90
290	0.3442	7.09	41.65	115.39	7.97
590	0.2218	1.98	26.84	74.36	2.23
990	0.1468	1.14	17.76	49.21	1.28
1990	0.0794	0.72	9.61	26.62	0.81
2990	0.063	0.62	7.62	21.12	0.70
5990	0.0505	0.52	6.11	16.93	0.58
9990	0.041	0.43	4.96	13.74	0.48
19990	0.0265	0.3	3.21	8.88	0.34
49990	0.0103	0.16	1.25	3.45	0.18
99990	0.0034	0.11	0.41	1.14	0.12

Table 4. Decay heat source in SNF canister and HWGL regions for codisposal WP filled to 75 % of SNF volume with melt-dilute ingot containing 100% Cs.

Storage Time (yrs)	Assembly Power (W/assembly)	Power per HWGL (W)	Total Power for SNF Can. (W)	Volumetric SNF Power (W/m ³)	Volumetric HWGL Power (W/m ³)
0	8.58	472.3	866.58	2881.11	530.91
10	6.53	375.99	659.53	2192.73	422.65
20	5.243	301.35	529.54	1760.56	338.75
50	2.83	159.5	285.83	950.30	179.29
90	1.382	73.1	139.58	464.07	82.17
190	0.487	16.81	49.19	163.53	18.90
290	0.3442	7.09	34.76	115.58	7.97
590	0.2218	1.98	22.40	74.48	2.23
990	0.1468	1.14	14.83	49.29	1.28
1990	0.0794	0.72	8.02	26.66	0.81
2990	0.063	0.62	6.36	21.15	0.70
5990	0.0505	0.52	5.10	16.96	0.58
9990	0.041	0.43	4.14	13.77	0.48
19990	0.0265	0.3	2.68	8.90	0.34
49990	0.0103	0.16	1.04	3.46	0.18
99990	0.0034	0.11	0.34	1.14	0.12

Table 5. Decay heat source in SNF canister and HWGL regions for codisposal WP filled to 50 % of SNF volume with melt-dilute ingot containing 100% Cs.

Storage Time (yrs)	Assembly Power (W/assembly)	Power per HWGL (W)	Total Power for SNF Can. (W)	Volumetric SNF Power (W/m ³)	Volumetric HWGL Power (W/m ³)
0	8.58	472.3	574.86	2866.84	530.91
10	6.53	375.99	437.51	2181.88	422.65
20	5.243	301.35	351.28	1751.85	338.75
50	2.83	159.5	189.61	945.59	179.29
90	1.382	73.1	92.59	461.77	82.17
190	0.487	16.81	32.63	162.72	18.90
290	0.3442	7.09	23.06	115.01	7.97
590	0.2218	1.98	14.86	74.11	2.23
990	0.1468	1.14	9.84	49.05	1.28
1990	0.0794	0.72	5.32	26.53	0.81
2990	0.063	0.62	4.22	21.05	0.70
5990	0.0505	0.52	3.38	16.87	0.58
9990	0.041	0.43	2.75	13.70	0.48
19990	0.0265	0.3	1.78	8.85	0.34
49990	0.0103	0.16	0.69	3.44	0.18
99990	0.0034	0.11	0.23	1.14	0.12

Table 6. Reference design conditions for the present thermal analysis.

Design Parameters	Design Conditions
<ul style="list-style-type: none"> • Back-filled gas inside / outside of SNF canister in codisposal WP 	<ul style="list-style-type: none"> • Helium gas inside and outside of SNF canister
<ul style="list-style-type: none"> • Transient decay heat loads for SNF and HWGL 	<ul style="list-style-type: none"> • 100% Cs melt-dilute (bounding LEU in Ref. 1) and DWPF canister design basis – See Table 2 to Table 5
<ul style="list-style-type: none"> • Initial reference time (storage time: "Year 0" in the present analysis) 	<ul style="list-style-type: none"> • 10 years' cooling time since discharge from reactor and production of HWGL
<ul style="list-style-type: none"> • Internal structure of the WP container 	<ul style="list-style-type: none"> • Intact codisposal geometry
<ul style="list-style-type: none"> • Repository ambient temperature 	<ul style="list-style-type: none"> • 100 °C
<ul style="list-style-type: none"> • Codisposal WP location in a repository tunnel 	<ul style="list-style-type: none"> • Center of a drift tunnel

5 Results and Discussions

Based on the approach methodology and the modeling assumptions, two-dimensional conduction model and conduction-radiation coupled model have been developed to investigate key parameters and to find sensitivities to the changes of the design parameters with respect to the reference conditions in relation to the thermal performance of intact codisposal waste package. The reference design conditions are shown in Table 6. The detailed model has also been developed to quantify the conservatism embedded in the baseline model and to investigate the detailed cooling mechanism internal to the codisposal WP. The CFD approach has been taken by using CFX [3] code as a tool to create prototypic geometry file under non-orthogonal mesh environment in the body-fitted coordinate system and to solve the non-linear conjugate equations by considering conduction, convection, and radiation cooling mechanisms and by using discrete radiation transport technique. In the previous report [1] the thermal performance analyses were made for the two options for aluminum-clad DOE SNF disposition using the codisposal WP design configuration. The two options are direct SNF disposal and melt-dilute disposition options. In the previous analysis decay heat loads of the melt-dilute disposition option were based on the assumption that 80% of the cesium isotopes were released during the melt-dilute process as shown Table 1.

The present thermal analyses are performed for the melt-dilute option only, that is, the codisposal WP containing the melt-dilute DOE SNF canister. 100% of the canister volume is filled with a uranium-aluminum alloy ingot. Thermal performance analyses of the codisposal WP containing 90%, 75%, or 50% volume melt-dilute SNF canister are also included in this report. These analyses will be useful in examining sensitivity of the WP peak temperature to the SNF volume fraction because metal ingot volume is dependent on the number of SNF assemblies processed in the melt-dilute option and different geometrical shape or size of melting crucible. The transient decay heat loads of the melt-dilute fuel inside the SNF canister are estimated by assuming that any cesium isotopes are not volatilized during the melting process. Tables 2 to 5 show the decay heat loads for 100, 90, 75, and 50 vol.% melt-dilute canisters as a function of storage time.

Aluminum-clad DOE SNF disposition by the melt-dilute technique is one of the alternate SNF treatment technology options. For this option, the aluminum based highly enriched uranium will be melted and diluted with U-238 to reduce the U-235 enrichment to 10 to 20%. In the melt-dilute disposition option, decay heat loads of the SNF canister of the codisposal WP will be dependent on how many assemblies will be melted and diluted in a DOE SNF canister. The majority of these assemblies will be Material Test Reactor (MTR) type such as aluminum-clad fuel. The decay heat source per each assembly processed in the melt-dilute option is the same as that of the assembly in the direct disposal option since it is assumed that melting will not release any of the Kr-85 and any fraction of cesium isotopes, Cs-134 and Cs-137 including Ba_m-137 daughter product. Decay heat source for HWGL will be the same as that of the direct disposal option.

The thermal performance analysis of the melt-dilute codisposal WP is conducted mainly by using the baseline model for the reference design conditions defined in Table 6. The analysis for the air-cooled WP is also performed during the first 2000 years of storage time. For the present analysis, two main cases are considered for the helium- and air-

cooled codisposal WP's with 100% cesium decay heat loads under various ambient temperatures of a repository using the intact codisposal WP configuration. One of the four cases considered here is the SNF canister filled with 100 vol.% of melt-dilute ingot corresponding to 135 fuel assemblies, and the others are the canisters filled with 90 vol.% of the ingot corresponding to 121 fuel assemblies, 75 vol.% to 101 assemblies, and 50 vol.% to 67 assemblies. All of them are 20% enriched alloy ingot containing the composition of aluminum-13.2 wt.% uranium. Table 7 shows thermal and radiation properties of the codisposal WP components containing the melt-dilute Al-SNF form ingot, which are used for the present analysis [1, 7, 8].

Table 7. Thermal and radiation properties of the codisposal WP components containing melt-dilute Al-SNF form used for the present analysis (Ref. 8).

Regions in Fig. 5	Materials		Thermal Conductivity	Emissivity
①	SNF Canister	Melt-Dilute Region	175.20 W/m K	—
		Canister Wall	17.30 W/m K	0.60
②	High-level Waste Glass Log (HWGL)		1.046 W/m K	0.60
③	Back-filled Gas	Helium	0.205 W/m K	—
		Air	0.036 W/mK	—
④	Co-Disposal Canister Inner Wall		10.977 W/m K	0.80
⑤	Co-Disposal Canister Outer Wall		48.810 W/m K	—

Thermal analysis has been performed for the melt-dilute codisposal WP by using the baseline model under the reference design conditions defined by Table 6. Typical radial temperature distributions over the entire region internal to the codisposal WP can be provided qualitatively by the previous results and the present analysis as shown in Fig. 9. The radial temperature distribution results of the He-cooled codisposal WP for the 100 vol.% SNF case are shown as a function of storage time in Fig. 10. Peak temperature at initial storage time ("0" year) is about 297 °C, and surface temperature of the WP is about 226 °C at zero year. Temperature gradients across the helium gas regions are much steeper than those of the other regions during the first 20 years of storage times. After 600 years of storage time, temperature of the WP actually becomes uniform over the entire region of the package. The results show that during the first 20 years of storage time radiation is the most dominant cooling mode among the three possible cooling mechanisms, which are conduction, convection, and radiation. In the analysis, the radiation properties are assumed to be independent of surface temperature although the amount of radiation emitted by a material surface partially depends on its temperature. Natural convective cooling mechanism is shown to be very weak since the WP container is emplaced horizontally in a geological repository. The level of contribution for each of the basic heat transfer mechanisms to the WP cooling may be indicated in terms of the dimensionless ratio of the temperature difference between the WP center and its wall boundary (θ_i , where $i = cond., conv., or rad.$). That is, using the notations defined by Fig. 9

$$\theta_{rad} = 100 \times \frac{(T_{m,1} - T_{m,2})}{(T_{m,1} - T_{wall})} \quad (15)$$

$$\theta_{conv} = 100 \times \frac{(T_{m,2} - T_{m,3})}{(T_{m,1} - T_{wall})} \quad (16)$$

$$\theta_{cond} = 100 \times \frac{(T_{m,3} - T_{wall})}{(T_{m,1} - T_{wall})} \quad (17)$$

For instance, at initial storage time of the He-cooled WP, the percentage contribution of the temperature difference between the WP center and its wall surface to each of the three cooling modes can be computed by using eqs. (15) to (17).

The results for 100 and 50 SNF volume percentages of the canister are shown in Table 8. The results show that convection contribution to the cooling of the present codisposal WP is negligible in predicting the peak temperatures of the present codisposal WP although it is very important in capturing non-uniform temperature effect of the waste package. It is also noted that radiation contribution decreases as total heat source decreases as a result of SNF volume reduction in the canister. Table 9 shows the level of radiative heat transfer effect on the coolability of the He-cooled 100 vol.% codisposal WP during the first 90 years of storage time since the emplacement of the codisposal WP in the repository. Figure 11 shows temperature contour plot for He-cooled 100% volume melt-dilute codisposal WP at 0 years of storage time based on the baseline model.

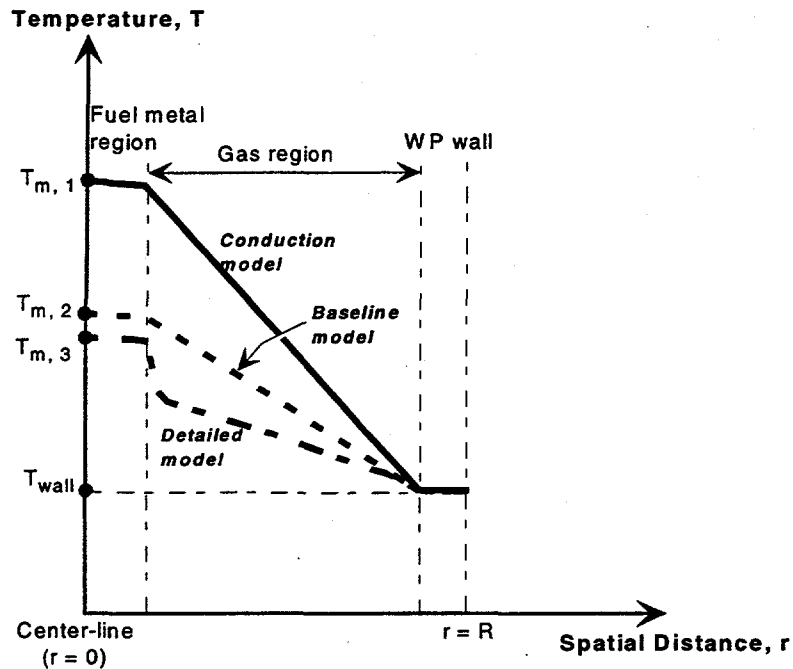


Figure 9. Qualitative temperature distributions predicted by the three models under the present codisposal WP configuration

Table 8. Typical levels of radiative cooling contributions to the thermal performance of the He-cooled-codisposal WP containing 100 vol.% and 50 vol.% melt-dilute SNF forms.

SNF volume %	θ_{rad} (Radiation)	θ_{cond} (Conduction)	θ_{conv} (Convection)
100	~ 74%	~ 25%	~ 1%
50	~ 61%	~ 37%	~ 2%

Table 9. Level of radiative cooling contribution to the thermal performance of the He-cooled codisposal WP containing 100 vol.% melt-dilute SNF form.

Storage Time (Years)	Peak Temperature of WP (°C)	θ_{rad} (defined by eq. (15)) (%)
0	297	74
10	266	69
50	177	62
90	142	52

The radial temperature distributions of the air-cooled codisposal WP for the 100 vol.% SNF case are shown as a function of storage time in Fig. 12. Peak temperature at initial storage time ("0" year) is about 302 °C, and surface temperature of the WP is about 230 °C at zero year. Temperature distribution inside the package becomes uniform along the radial direction near the 200 years of storage time. Figure 13 shows temperature contour plot over the entire computational domain of air-cooled 100 vol.% codisposal WP based on the baseline model results at 0 years of storage time.

Table 10 presents quantitative comparison of peak temperatures between He-cooled and air-cooled codisposal packages with 100 vol.% SNF canister containing 100 %Cs in melt-dilute ingot as a function of storage year. Figure 14 shows graphical comparison of peak temperatures between the two different back-filled packages as a function of storage time. Table 11 shows peak temperatures for various volume percentages of melt-dilute forms using 20 %Cs and 100%Cs decay sources. It is noted that the peak temperature difference between the two packages under 100 vol.% SNF WP is small compared to the other designs containing the SNF canister less than 100 vol.% SNF. This is mainly due to the presence of high thermal conductivity region of metal ingot in the melt-dilute SNF canister instead of back-filled gas region in the direct Al-SNF canister. Figure 15 shows comparison of non-dimensional temperature distributions between two WP design options, melt-dilute and direct Al-SNF forms, for 50 and 100 vol.% of SNF in the WP. Table 12 shows quantitative comparison between the two SNF disposal forms in terms of maximum temperature difference across the entire region internal to the codisposal WP.

Table 10. Comparison of peak temperatures for the codisposal WP with 100 vol.% SNF canister containing 100% Cs in melt-dilute alloy ingot based on the baseline model for various storage times (ambient temperature = 100 °C).

Storage Times (Years)	Melt-Dilute WP (100 vol.%)	Melt-Dilute WP (100 vol.%)
	He-filled WP	Air-filled WP
0	297	301
10	266	269
20	235	239
50	177	181
90	142	148
190	110	113
590	100	102
1990	100	100

Table 11. Comparison of peak temperatures for the He-cooled codisposal WP with various volume percentages of SNF canister containing 20% Cs and 100% Cs in melt-dilute alloy ingot based on the baseline model for various storage times (ambient temperature = 100 °C).

Storage Times (Years)	Melt-Dilute WP (75 vol.% SNF)	Melt-Dilute WP (90 vol.% SNF)	Melt-Dilute WP (100 vol.% SNF)
	20% Cs decay load	20% Cs decay load	100% Cs decay load
0	284 (347*)	264 (286*)	297(301*)
10	247	238	266
50	168	168	177
90	135	133	142
190	115	107	110
590	104	101	100
1990	102	100	100

Note: * Peak temperature for the air-filled WP.

Table 12. Comparison of peak and wall temperatures for the He-cooled and air-cooled codisposal packages with 50 and 100 volume percentages of SNF canister containing 100% Cs in melt-dilute alloy ingot based on the baseline model at 0 years of storage times under the reference design conditions of Table 6.

Max. and WP Wall Temperatures	Direct SNF form		Melt-Dilute SNF form		
	He-filled 50 vol.%	Air-filled 50 vol.%	He-filled 50 vol.%	He-filled 100 vol.%	Air-filled 100 vol.%
Max. Temperature (°C)	304	466	293	297	301
WP Wall Temperature (°C)	206	206	206	226	227
ΔT *(°C)	98	260	87	71	74

Note: * Max. temperature difference of WP = (Max. temperature – WP wall temperature)

Sensitivity calculations of the WP peak temperatures with respect to the four melt-dilute ingot volume percentages (50%, 75%, 90%, 100%) of the SNF canister were performed at 0 years of storage time under the reference design conditions of Table 6. When volume fraction of the metal ingot to the SNF canister decreases from 100 vol.% to 50 vol.%, total decay heat load of the ingot decreases from 577 watts to 482 watts as shown in Table 13, but back-filled gas volume inside the canister increases. The thermal performance results at 0 years of storage time are summarized in Table 13. When metal ingot volume decreased to 90 vol.%, maximum temperature of the WP containing the 90 vol.% ingot SNF canister was 301 °C at 0 years of storage time. This result is 4 °C higher than that of the 100 vol.% WP as a result of the offset effect of SNF heat source decrease and back-filled gas volume increase due to ingot volume reduction inside the SNF canister. Figure 16 shows comparison of maximum temperatures for He-cooled melt-dilute codisposal WP's for various ingot volume percentages of the SNF canister at 0 years of storage time.

Table 13. Comparison of peak and wall temperatures for the He-cooled codisposal WP with various volume percentages of SNF canister containing 100% Cs in melt-dilute alloy ingot based on the baseline model at 0 years of storage times under the reference design conditions of Table 6.

Max. and WP Wall Temperatures	50 vol.%	75 vol.%	90 vol.%	100 vol.%
SNF Decay Load (W)	482	530	557	577
Max. Temperature (°C)	293	298	301	297
WP Wall Temperature (°C)	206	216	226	226
ΔT *(°C)	87	82	75	71

Note: * Max. temperature difference of WP = (Max. temperature – WP wall temperature)

In Fig. 17, non-dimensional temperature distributions for various volume fractions of SNF ingot volumes are shown along the radial direction from the center of the codisposal WP to the boundary wall region. It is clearly shown in Fig. 17 that back-filled gas region of the SNF canister has steep temperature gradient due to sudden change of thermal conductivity at the interface of metal ingot and gas regions for the ingot volume percentages less than 100%. Although the codisposal WP containing 100 vol.% SNF is the most efficient design for SNF disposal in terms of thermal performance viewpoint, it is expected to have non-zero fraction of gas volume inside the canister because in reality the ingot surface may not contact the inner wall of the SNF canister completely, or gas bubbles may be trapped into the ingot during the melting and dilution process. Figure 18 shows temperature contour plot for the codisposal WP containing 90 vol.% filled SNF canister, which has the highest peak temperature among the four different ingot vol.% of the canister.

Table 14 shows comparison of peak temperatures for He-cooled codisposal WP with two different volume percentages (90% and 100%) of SNF canister containing 100% Cs in melt-dilute alloy ingot at 0 years of storage time under various ambient temperatures. The results were obtained by using the baseline model. Under the reference conditions, peak temperatures of the codisposal WP were found to be 297 and 301 °C for 100 and 90 volume percentages of the canister, respectively. Figure 19 presents the graphical results for various geological temperatures around the WP. It is noted that peak temperature difference between He-cooled and air-cooled 90 vol.% WP designs is 25 °C higher than that of the 100 vol.% filled WP's for the 10 vol.% increase of the back-filled gas volume in the canister. Figure 20 shows comparison of temperature distributions for He-cooled 100 vol.% and 90 vol.% melt-dilute WP's along the A-A' line shown in the same figure at 0 years of storage time using the baseline model with 150 °C of geological ambient temperature. The graphical results in Fig. 20 show about 4 °C increase in peak temperature due to the additional temperature drop across the helium gap corresponding to 10% of the SNF canister volume for the same boundary conditions.

As shown in Fig. 21, maximum temperature differences between the air-cooled WP and the He-cooled WP are about 2 to 4 °C for various geological ambient temperatures at initial storage period of the 100 vol.% melt-dilute WP design. In this case the temperature levels are high enough such that the radiation cooling mode is dominant compared to the conductive cooling mechanism in the back-filled gas medium as

discussed earlier. The SNF canister and the five HWGL's in an enclosed WP container are also assumed to have diffuse-gray surfaces with no absorption or emission by the intervening back-filled gas medium. Therefore, the difference of thermal conductivity between air and helium gases may cause little impact on the peak temperature predictions although thermal conductivity of helium gas is about six times higher than that of air. The quantitative results for the He-cooled and air-cooled codisposal WP's containing 100 vol.% SNF canister with decay source of 100% Cs are shown in Table 15.

Table 14. Comparison of peak temperatures for the He-cooled codisposal WP with two different volume percentages of SNF canister containing 100% Cs in melt-dilute alloy ingot based on the baseline model for various ambient temperatures at 0 years of storage time.

Ambient Temperature (°C)	Melt-Dilute WP (90 vol.% SNF)	Melt-Dilute WP (100 vol.% SNF)
	100%Cs decay load	100%Cs decay load
50	267	262
100	301 (330*)	297 (301*)
150	339	333
200	378	371

Note: * Peak temperature for the air-filled WP.

Table 15. Comparison of peak temperatures for the He-cooled and air-cooled codisposal WP's with 100 volume percentage of SNF canister containing 100% Cs in melt-dilute alloy ingot based on the baseline model for various ambient temperatures at 0 years of storage time.

Ambient Temperature (°C)	Melt-Dilute WP (100 vol.% SNF with 100%Cs decay)	
	He-filled WP	Air-filled WP
50	262	266
100	297	301
150	333	335
200	371	373

Comparison of the radial temperature distributions between the baseline model and the conduction model are made in Fig. 22. The graphical results show that radiative cooling mechanism is most dominant among the possible cooling modes as shown in Table 8. For less than about 130 °C of the WP peak temperature, the radiative energy transfer is found to be small compare to other cooling modes.

Comparison of the three model results along the vertical centerline is shown in Fig. 23. The results from the detailed model show that the temperature at the top surface of the WP is about 10 °C higher than the WP bottom temperature because hot gas tends to move upward due to the gravitational effect. These results are very similar to those of the direct AL-SNF form WP documented in the previous report [1]. On the other hand,

the baseline model can not capture this physical behavior due to neglect of the natural convection mechanism even though it predicts the maximum temperature similar to that of the detailed model. Figure 24 shows radial temperature distributions performed by the two models along the near-horizontal line of SNF center to HWGL center (A-A' line shown in the same figure). From these results, temperature gradient across the HWGL region for the detailed model is much smaller than that of the baseline model due to the gas temperature mixing effect driven by the natural gas circulation inside the WP.

Figure 25 shows velocity vector plot over the flow domain of back-filled gas inside the direct codisposal WP for the reference conditions. Temperature contour plot corresponding to the velocity distribution of Fig. 25 is shown in Fig. 26. This information may be important in predicting the movement of humidity and condensate water sources around the surface of the WP container, which can be closely related to the corrosion or degradation model of the codisposal WP. The gas flow pattern over the entire flow domain within the WP container is illustrated in Fig. 27 from the computational results under the reference design conditions (He-cooled codisposal WP with 100% Cs decay heat source).

It is emphasized that all the present analyses are performed using 100% Cs decay heat load for the melt-dilute alloy ingot, which is located inside the SNF canister of the codisposal WP. This transient decay heat load is estimated in a conservative way by assuming that any cesium isotopes are not released during the melt-dilute process.

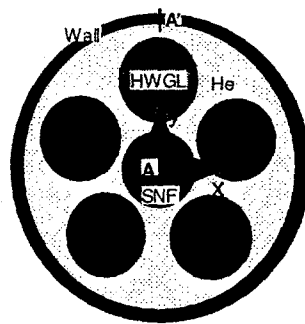
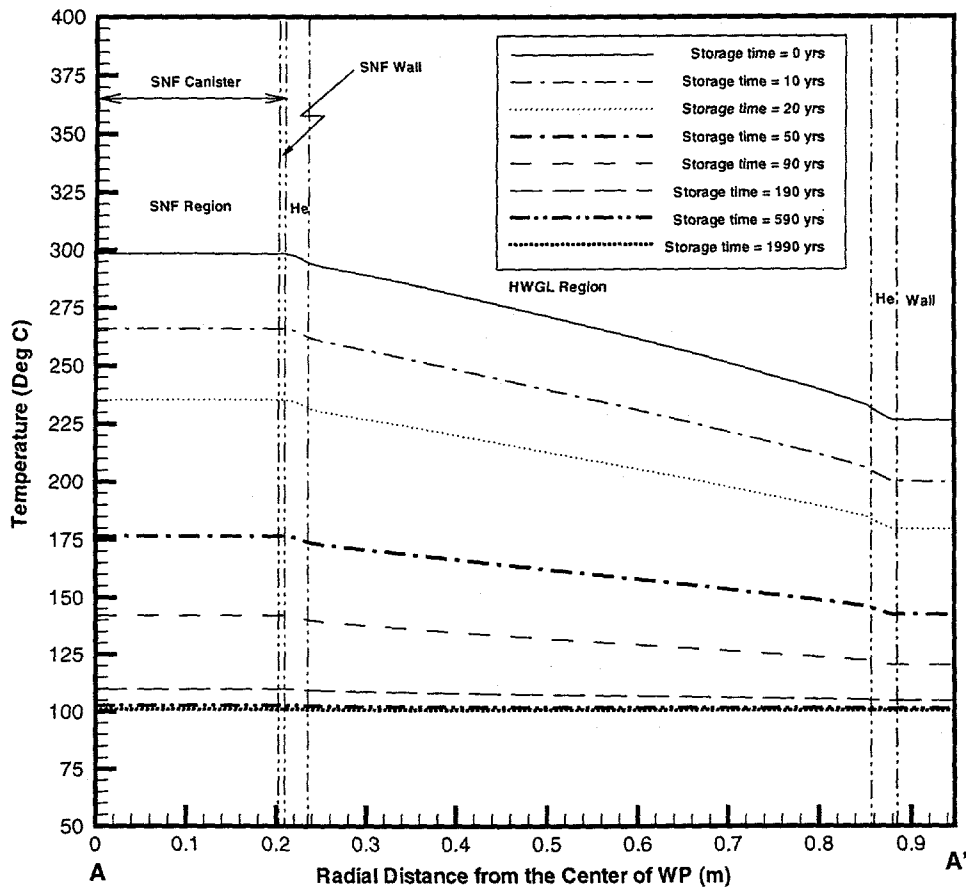
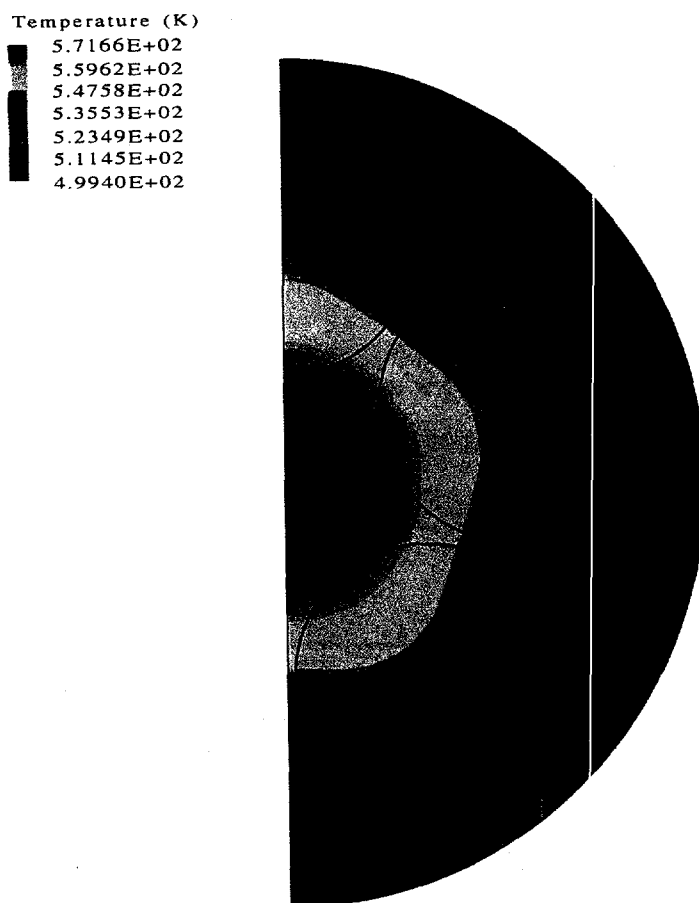


Figure 10. Radial temperature distribution of He-cooled 100% volume melt-dilute codisposal WP for various storage times based on the baseline model.



He-cooled 100vol% Melt-Dilute SNF Canister

Figure 11. Temperature contour plot for He-cooled 100% volume melt-dilute codisposal WP based on the baseline model at 0 years of storage time.

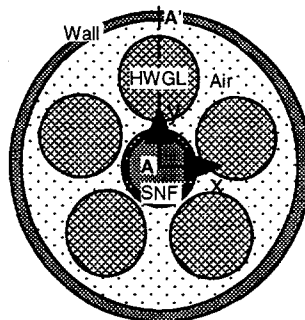
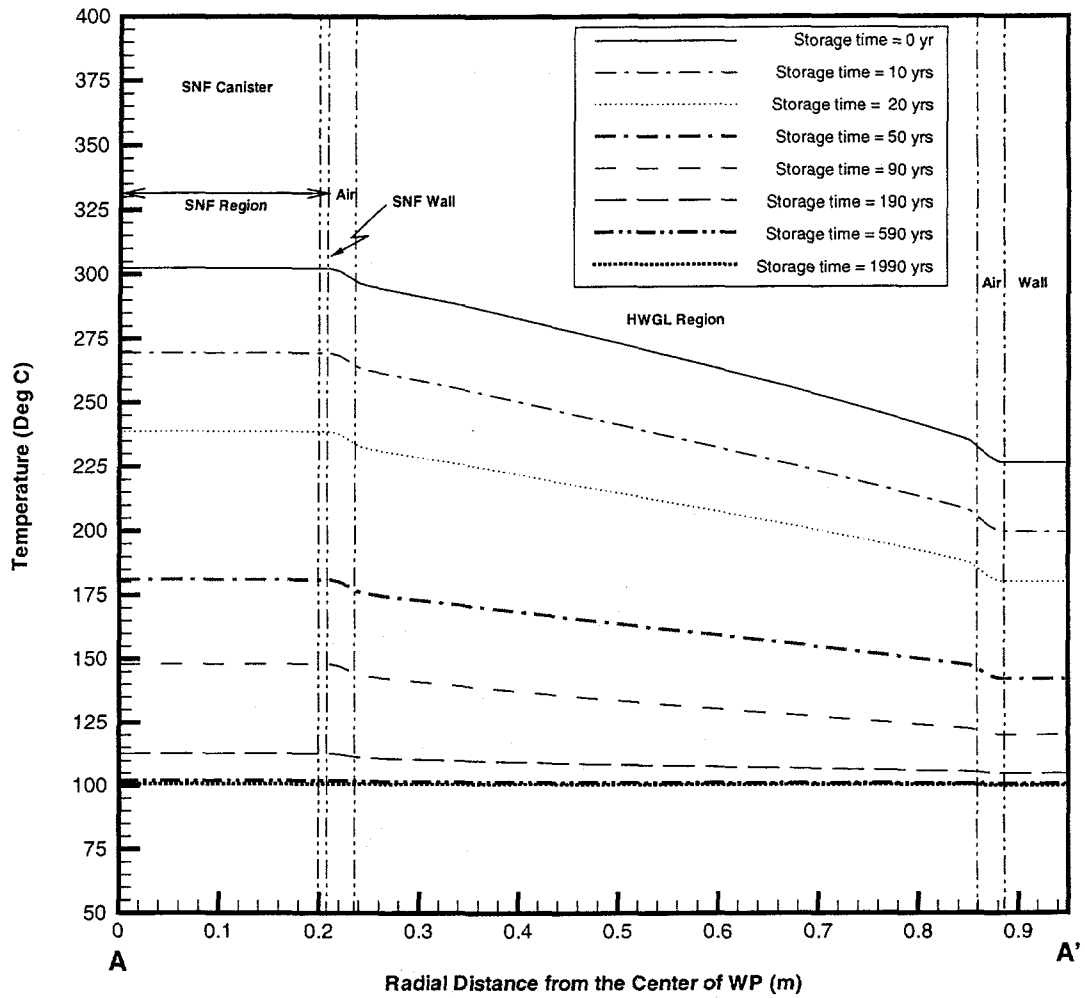
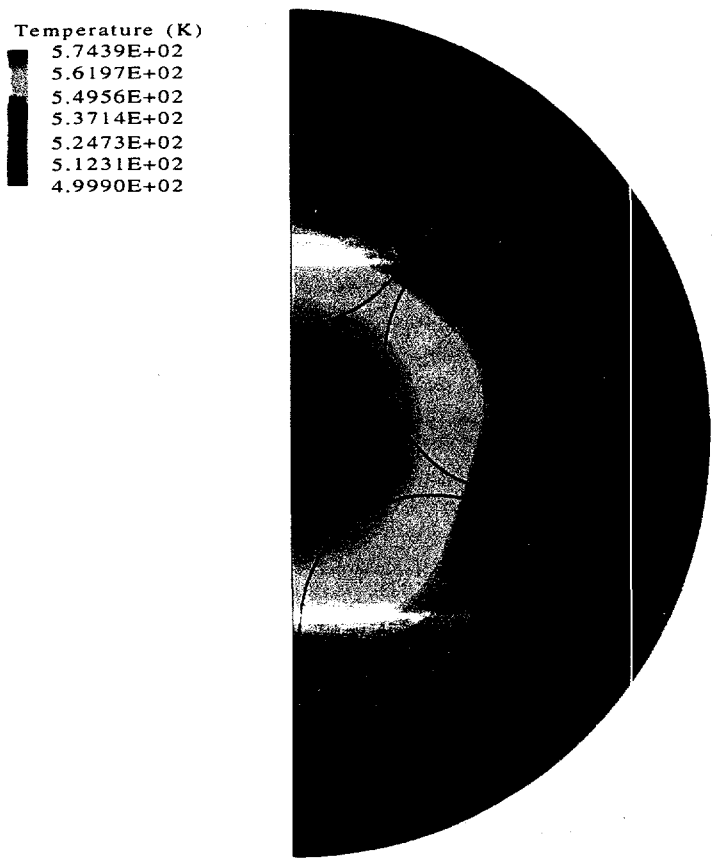


Figure 12. Radial temperature distribution of Air-cooled 100% volume melt-dilute codisposal WP for various storage times based on the baseline model.



Air-cooled 100 vol% Melt-Dilute SNF canister

Figure 13. Temperature contour plot for air-cooled 100% volume melt-dilute codisposal WP based on the baseline model at 0 years of storage time.

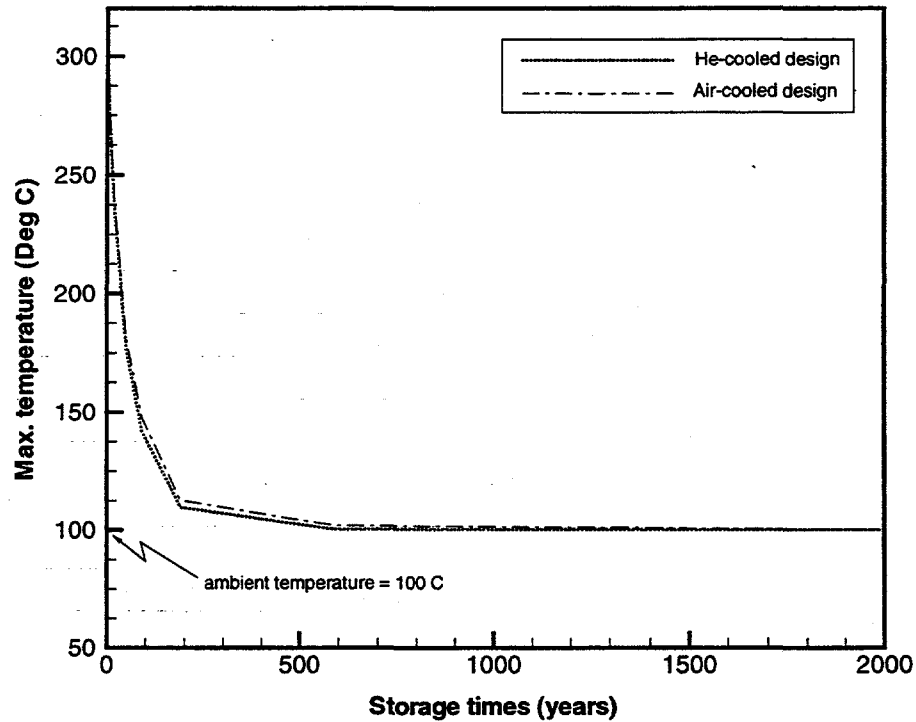
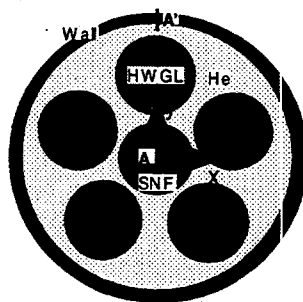
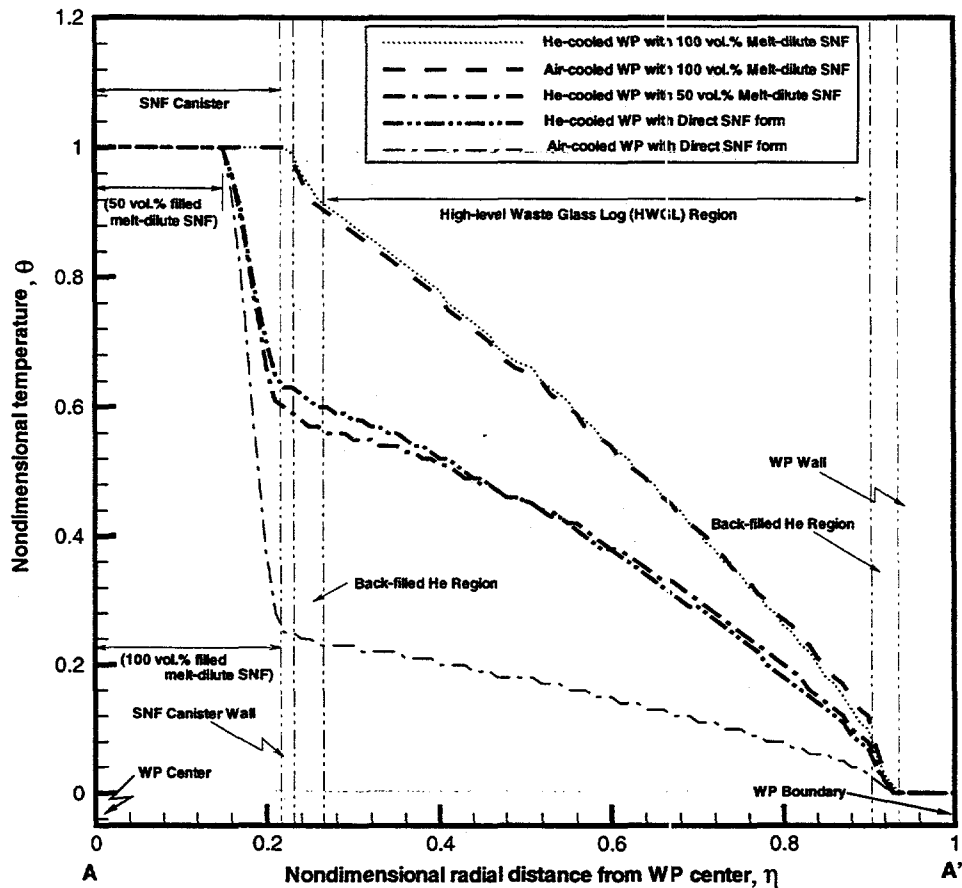


Figure 14. Comparison of maximum temperatures for He-cooled and air-cooled 100% volume melt-dilute codisposal WP's for various storage times based on the baseline model.



$$\theta = \frac{(T - T_{wall})}{(T_{max} - T_{wall})}, \quad \eta = \frac{r}{R}$$

(The parameters used in θ and η are defined in Fig. 9.)

Figure 15. Non-dimensional radial temperature distributions for He-cooled melt-dilute and direct Al-SNF codisposal WP's for 50 and 100 volume percentages of SNF based on the baseline model at 0 years of storage time.

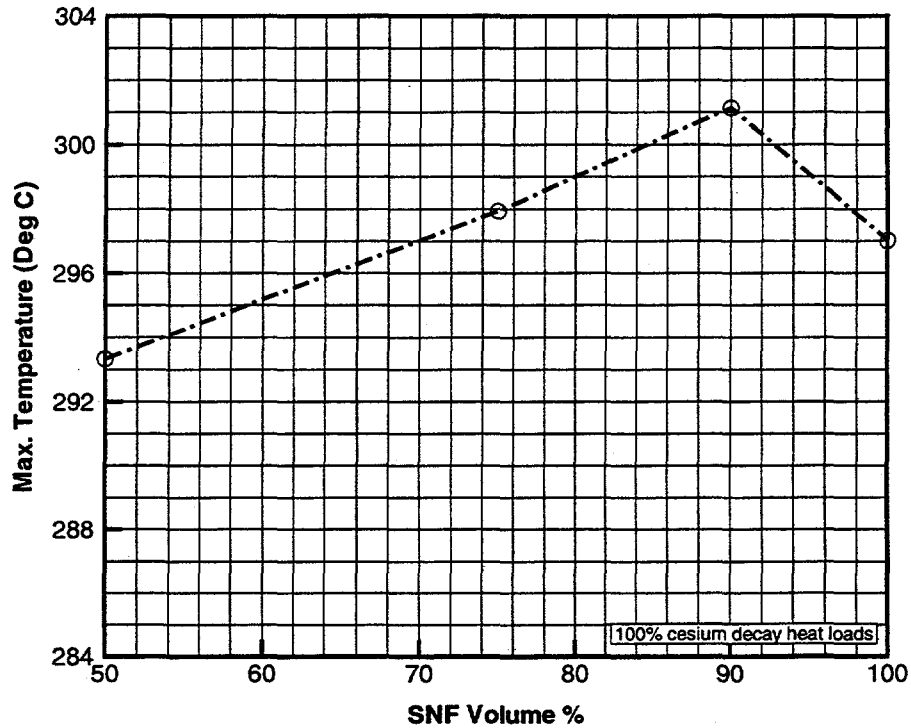
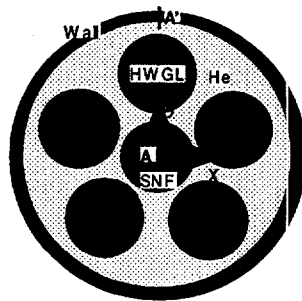
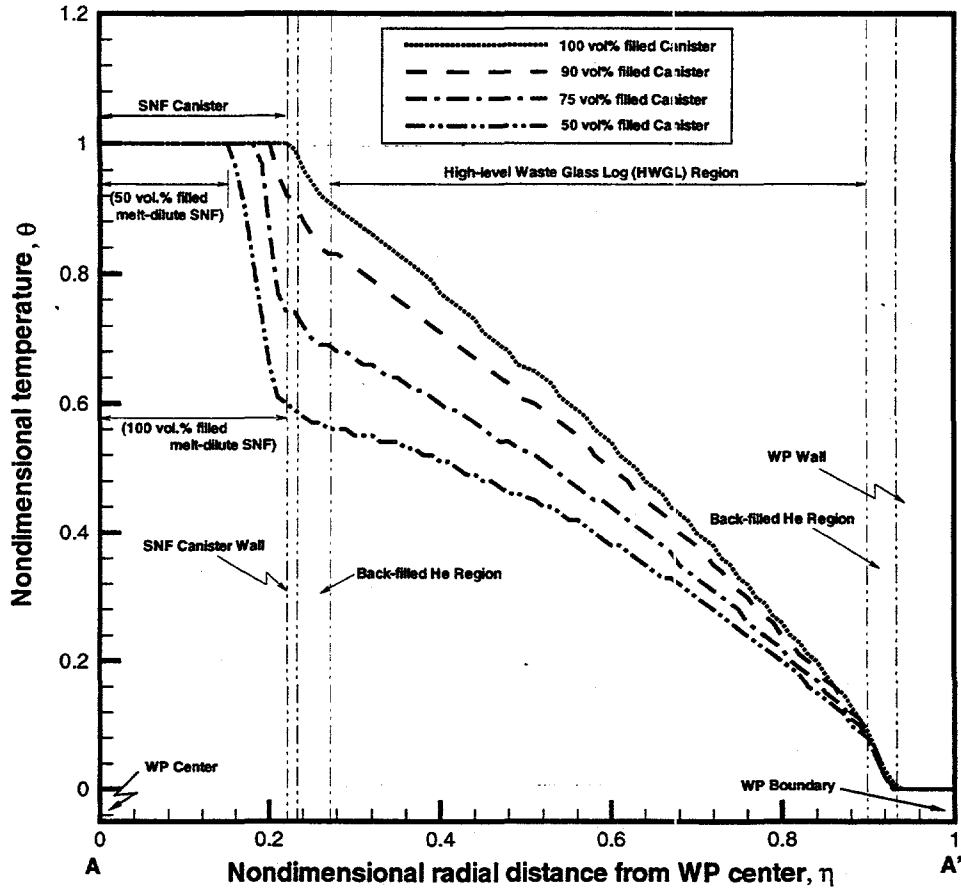
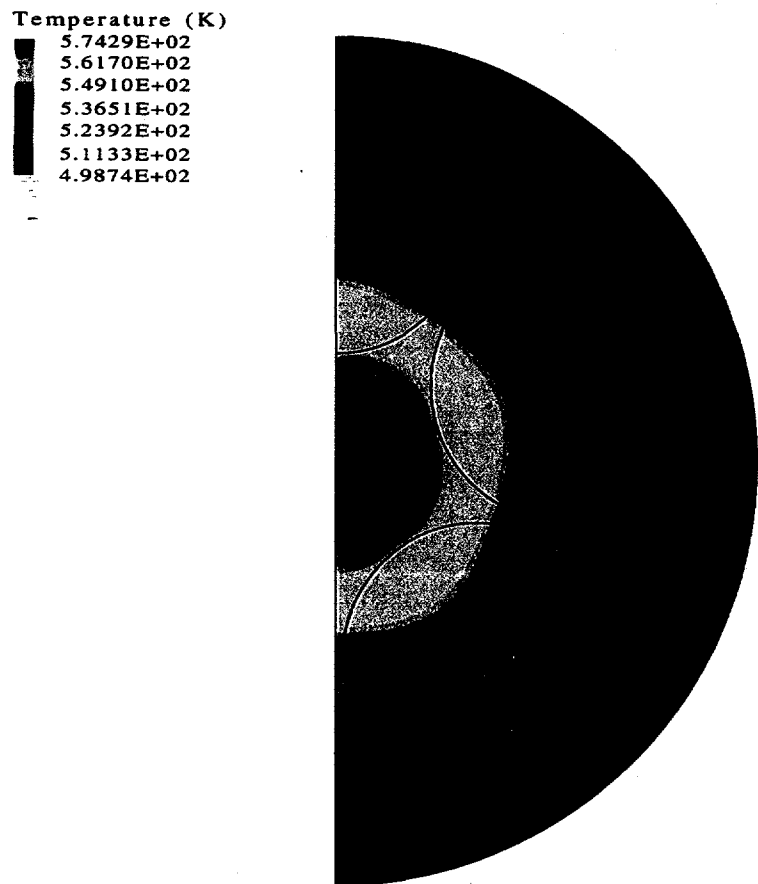


Figure 16. Comparison of maximum temperatures for He-cooled melt-dilute codisposal WP's for various ingot volume percentages of the SNF canister at 0 years of storage time based on the baseline model.



$$\theta = \frac{(T - T_{wall})}{(T_{max} - T_{wall})}, \quad \eta = \frac{r}{R} \quad (\text{The parameters used in } \theta \text{ and } \eta \text{ are defined in Fig. 9.)}$$

Figure 17. Non-dimensional radial temperature distribution for He-cooled melt-dilute codisposal WP for various volume percentages of SNF based on the baseline model at 0 years of storage time.



He-cooled 90 vol% Melt-Dilute SNF Canister

Figure 18. Temperature contour plot for He-cooled 90% volume melt-dilute codisposal WP based on the baseline model at 0 years of storage time.

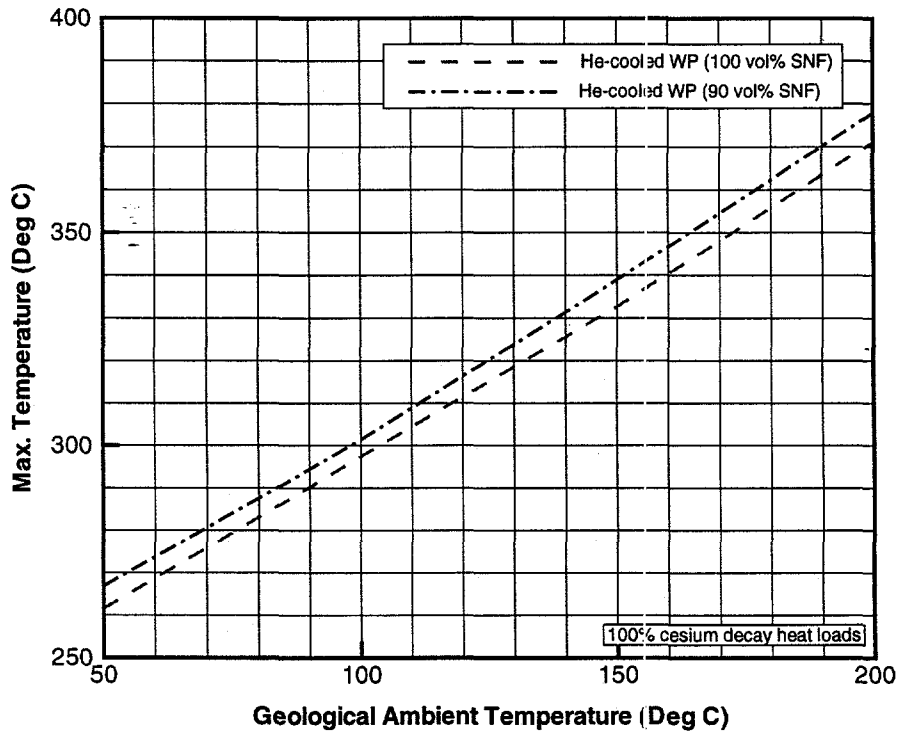


Figure 19. Comparison of maximum temperatures for He-cooled 100% and 90% volume melt-dilute codisposal WP's for various geological ambient temperatures based on the baseline model.

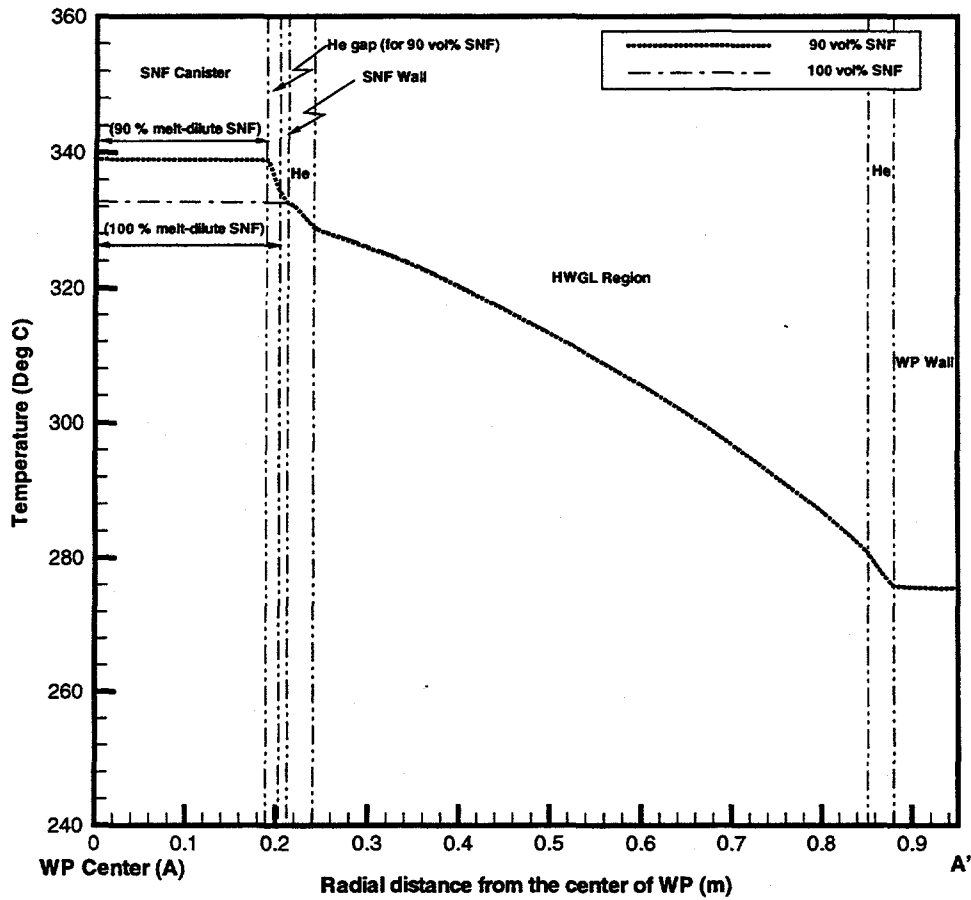


Figure 20. Comparison of radial temperatures for He-cooled 100% and 90% volume melt-dilute codisposal WP's for 0 year's initial reference storage time based on the baseline model (ambient temperature = 150 °C).

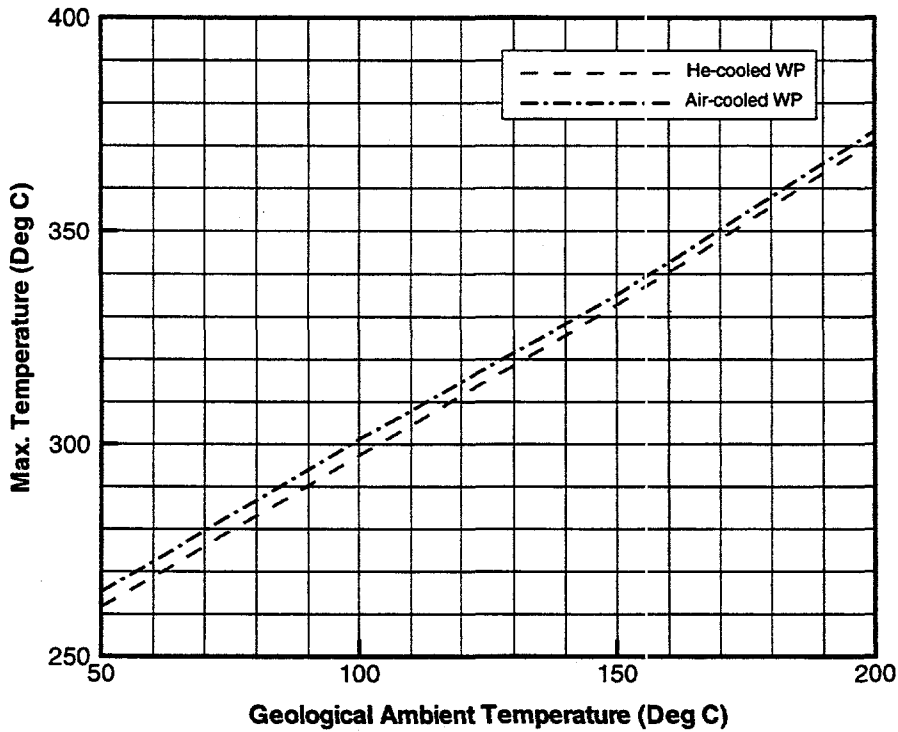


Figure 21. Maximum temperatures of air-cooled and helium-cooled 100 vol% melt-dilute codisposal waste packages with bounding SNF decay heat loads for various geological ambient temperatures.

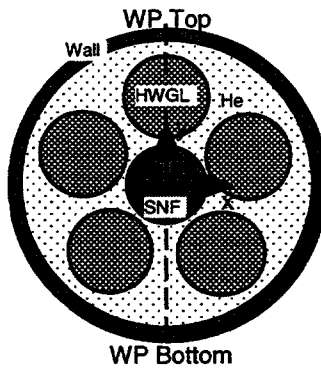
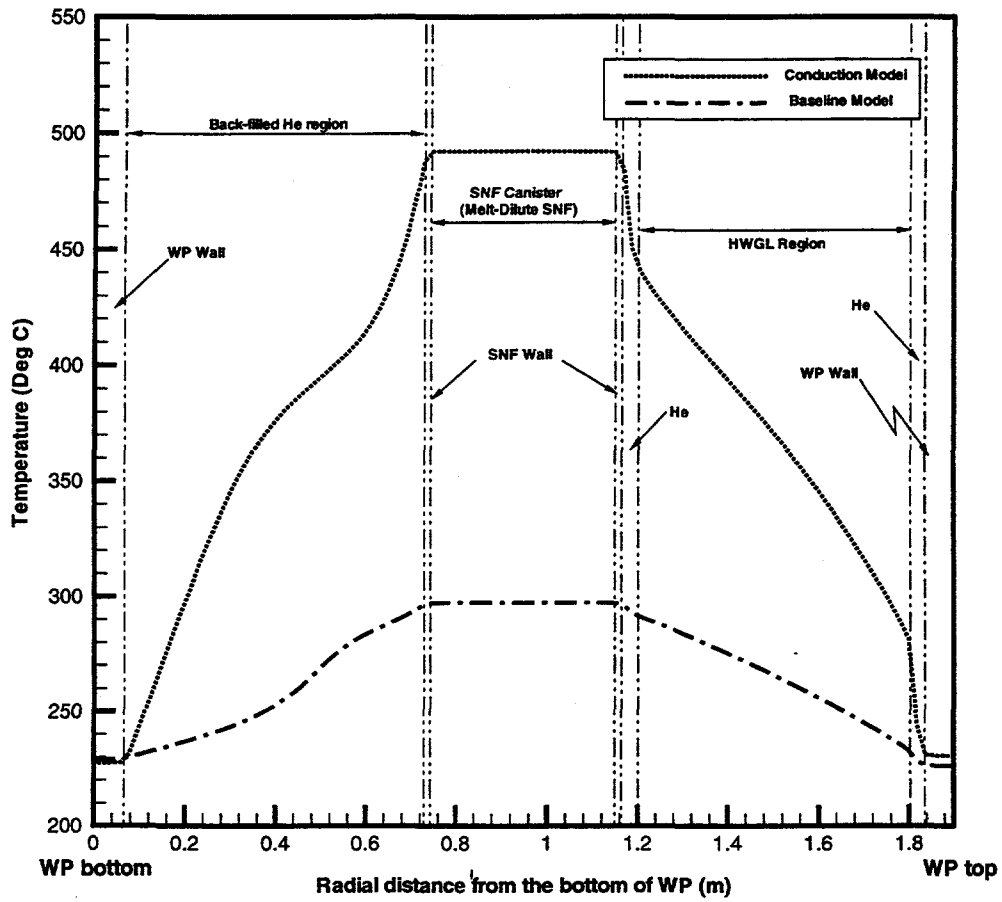


Figure 22. Comparison of centerline temperature distributions based on the baseline model and the conduction model for helium-cooled 100 vol% melt-dilute codisposal WP with 100% Cs decay heat source.

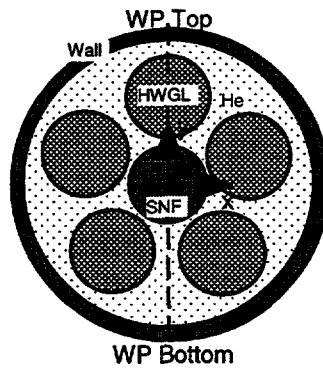
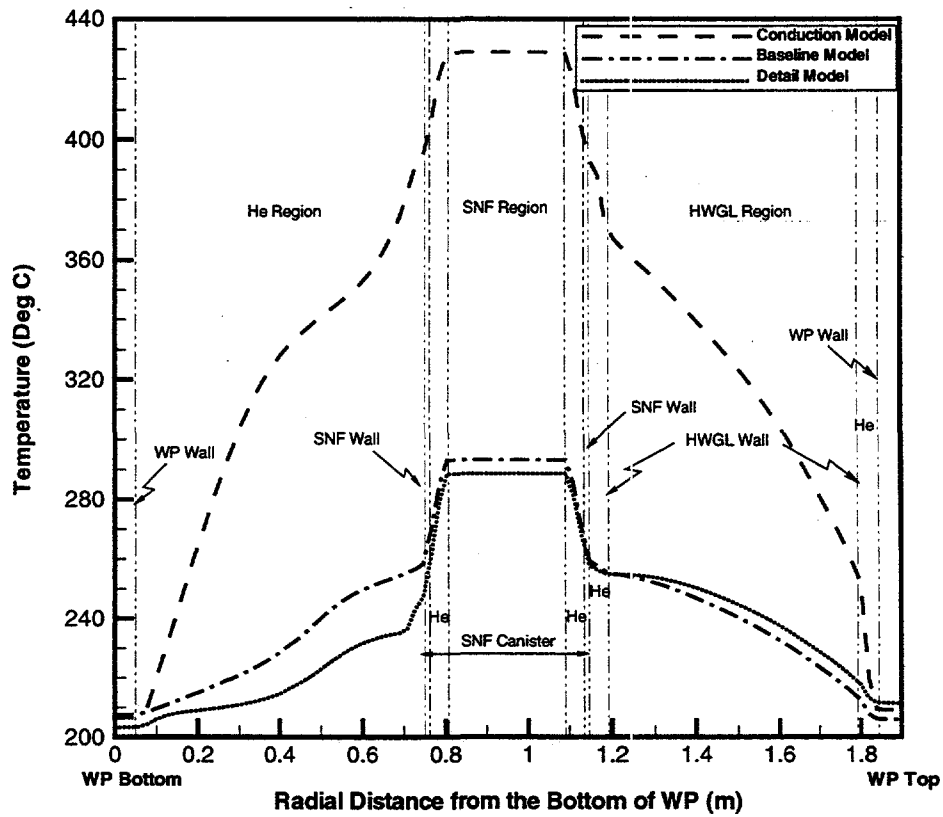


Figure 23. Comparison of centerline temperature distributions based on the baseline model, the conduction model, and the detailed model for helium-cooled 50 vol% melt-dilute codisposal WP with 100% Cs decay heat source at 0 years of storage time.

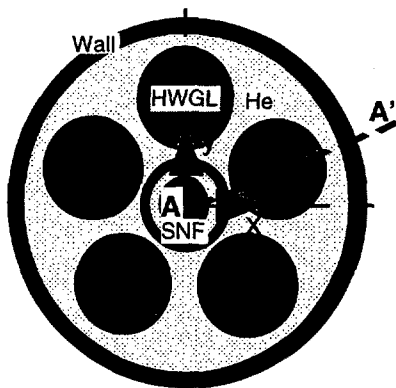
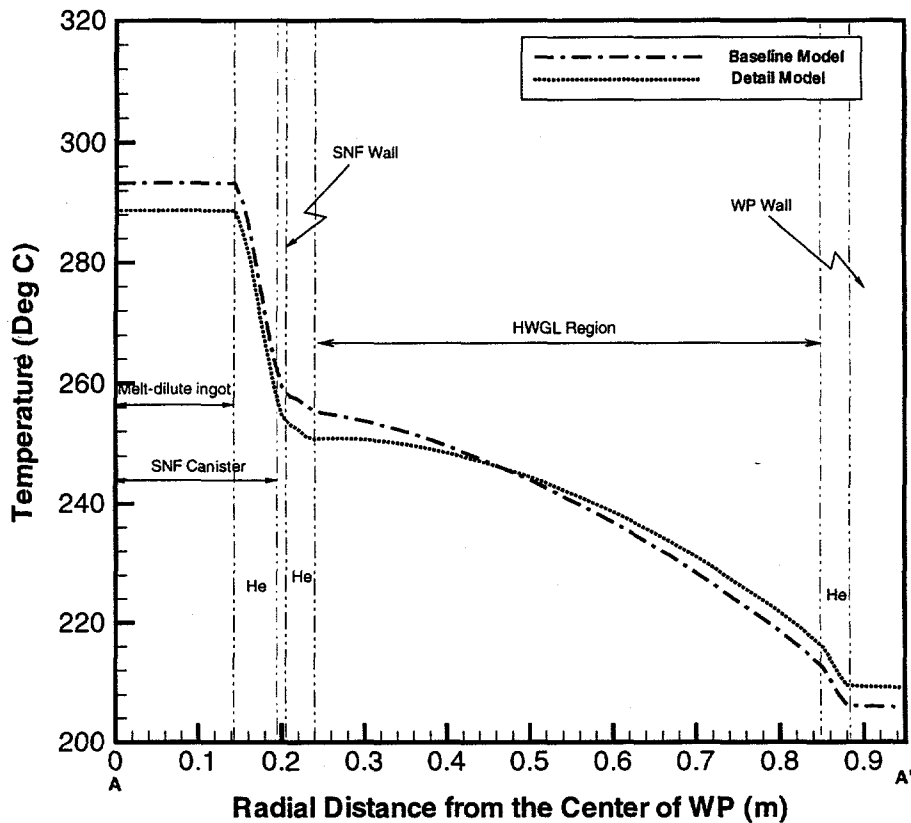
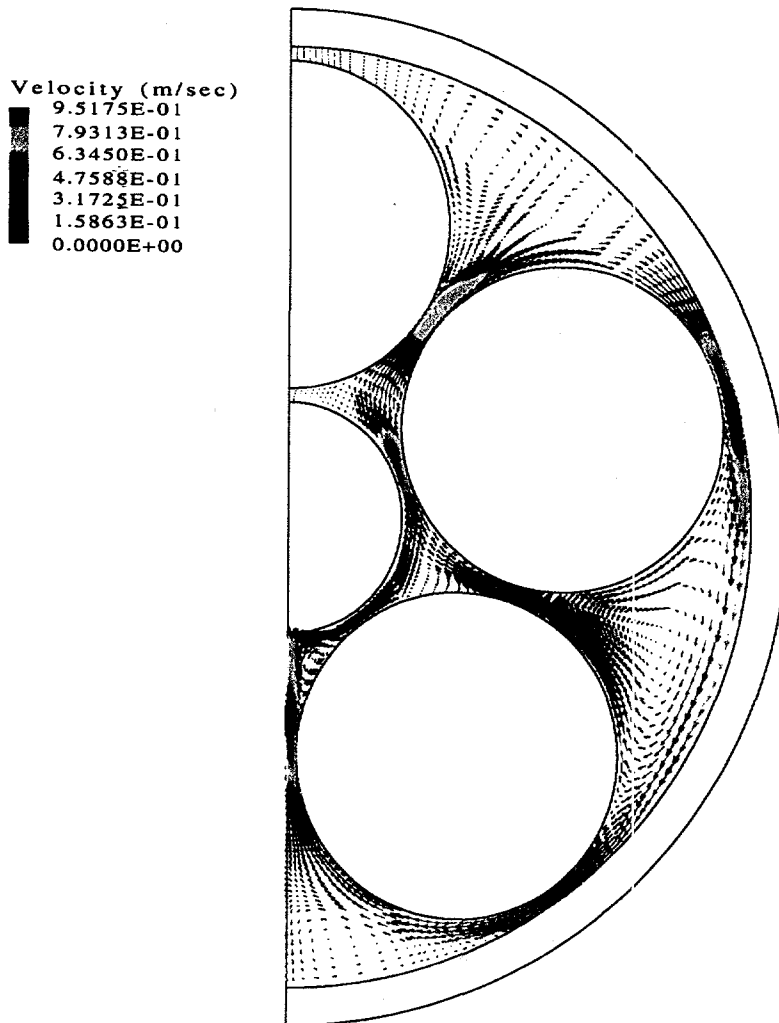


Figure 24. Comparison of radial temperature distributions along the line A-A' based on the baseline model and the detailed model for helium-cooled direct codisposal WP with with 100% Cs decay heat source at 0 years of storage time.

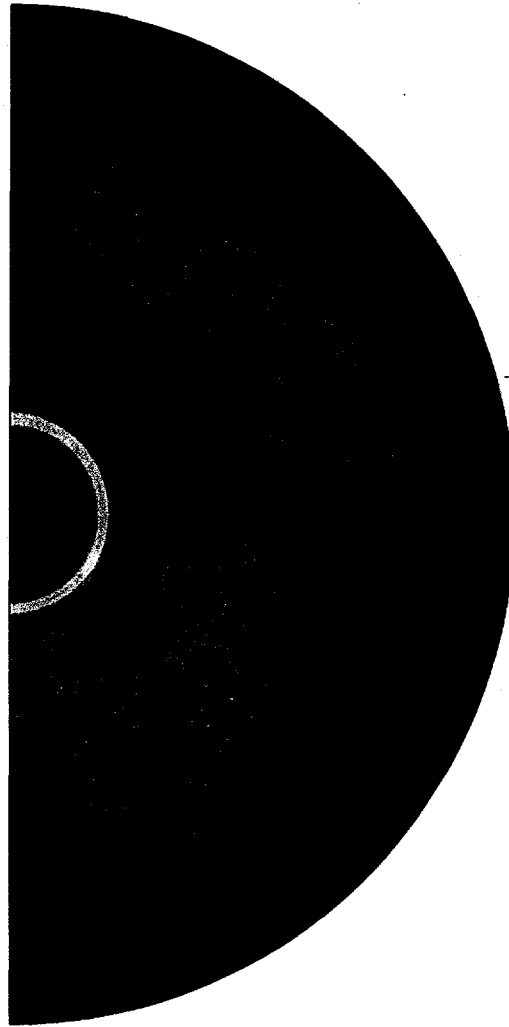


Conduction, radiation, and convection (50 vol.% and 100 %Cs)

Figure 25. Velocity vector plot of back-filled gas motion due to natural convection based on the detailed model for helium-cooled 50 vol% melt-dilute codisposal WP with 100% Cs decay heat source at 0 years of storage time.

Temperature (K)

■	5.6185E+02
■	5.4756E+02
■	5.3327E+02
■	5.1898E+02
■	5.0468E+02
■	4.9039E+02
■	4.7610E+02



Conduction, radiation, and convection (50 vol.% and 100 %Cs)

Figure 26. Temperature contour plot over the entire computational domain based on the detailed model for helium-cooled 50 vol% melt-dilute codisposal WP with 100% Cs decay heat source at 0 years of storage time.

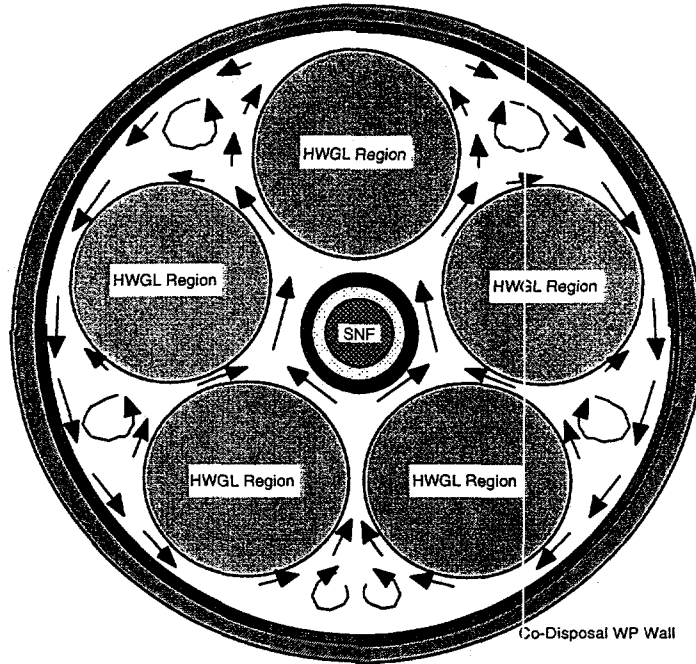


Figure 27. Back-filled gas flow pattern due to natural convective cooling within codisposal waste package.

6 Conclusions

Three thermal models have been developed to assess the thermal performance of the codisposal WP design using intact prototypic geometry created under the body-fitted coordinate system in the CFD preprocessing environment. They are the conduction model, the baseline model considering conduction-radiation coupled heat transfer mechanisms, and the detailed model including all three possible modes such as conduction, convection, and radiation energy transport modes [1].

The present analysis mainly used the baseline model with well-defined decay heat loads for the SNF canister and HWGL regions internal to the codisposal WP. The conduction model was also used to identify dominant cooling mechanism under the present codisposal WP configuration. Reference design boundary conditions were provided to the analysis model from the WP performance requirements of a drift tunnel repository. In this report, the melt-dilute form options, which have been recently evolved since the first repository thermal analysis report [1] was completed, were considered for the alternative SNF treatment program using the codisposal WP configuration. The two-dimensional thermal performance analyses for various melt-dilute design conditions under the present codisposal WP configuration were made mainly using the baseline model because of a computational efficiency. Estimation of the SNF decay heat source for the analysis was based on the conservative assumption that any fraction of cesium isotopes would not be removed during the melt-dilute process of Al-SNF form.

However, the detailed model was used to investigate the physical heat transfer mechanism inside the codisposal WP container in detail under the reference design conditions defined in Table 6. In addition, the results of the detailed model provided quantitative estimation of the conservatism imbedded in the baseline model. The detailed model gave highly non-uniform package wall surface temperature such that top surface temperature of the WP is about 10°C higher than that of the WP bottom surface. On the other hand, as shown in Fig. 23, the baseline model results showed that top surface temperature is about the same as the bottom surface temperature of the WP due to the neglect of buoyancy-driven internal gas circulation although the baseline model prediction of the WP peak temperature is slightly higher than that of the detailed model. The detailed model results also showed that temperature gradients across the HWGL regions are much smaller compared to the predictions of the baseline model for a given elevation height from the bottom of the WP under the present storage configuration. This is one of the evidences of the buoyancy-driven circulation internal to the codisposal WP. This phenomenon may be important in relation to the movement of water moisture around the WP surface inside a drift tunnel since the moisture directly affects corrosion of the WP materials. Peak temperatures with the detailed model are about 5°C lower than the baseline model. From the results of the conduction model, the radiative cooling process is shown to be the most dominant mode among the three possible heat transfer modes for higher than 130°C of the peak package temperature under the present WP configuration although cooling mechanisms are quite different one another.

Thermal performance analyses of the codisposal WP containing four different volume fractions of metal ingot in the canister (50 to 100 vol.%) were made using the baseline model under the reference conditions shown in Table 6. When the ingot volume fraction of the canister is 90 vol.%, peak temperature of the He-cooled WP at 0 years of storage

time is the largest among the four different ingot volume WP design options as shown in Fig. 16.

The results of the baseline model showed that 100 and 90 vol.% filled melt-dilute disposition options for the helium-filled and air-filled WP's satisfied the present waste acceptance criteria for the WP design under the reference boundary conditions in terms of the peak temperature criterion, $T_{\max} \leq 350$ °C. Assessment of several melt-dilute Al-SNF disposition options with 100% Cs decay heat load has been completed. It should be emphasized that the results were based on the natural convective cooling mechanism without any help of external or forced circulation devices around the WP boundary. In addition, 10 years' cooling time for the decay heat loads of the SNF and HWGL regions was used for the present analysis as one of the reference design conditions, but in reality the time for the WP to leave waste custodian and then to be transported to a repository site may be much longer than 10 years.

7 Recommendations

The present work used a sensitivity analysis approach with respect to the reference design conditions. The baseline model/analysis tool should be used to assess the thermal performance of evolving and confirmed WP designs using better-defined geological boundary conditions to demonstrate compliance to the repository waste acceptance criteria.

The following recommendations are made for the improvement of the baseline model:

- The present analysis used intact codisposal waste package with no internal structures to support SNF and waste glass logs since final geometrical configuration is neither confirmed nor available yet. The future model needs to include internal structure of the codisposal package to find out any impacts on the assessment of the WP thermal performance for the long-term storage.
- This report deals with the thermal performance internal to the codisposal WP. The thermal analysis modeling of hydro-geological media surrounding the WP, including the geological drift tunnel region, needs to be included to accurately model the repository temperature history. This would include the effects of water or humidity of a drift tunnel region outside the codisposal WP.

8 References

1. S. Y. Lee and R. L. Sindelar, "Thermal Analysis of Repository Codisposal Waste Packages Containing Aluminum Spent Nuclear Fuel (U)", WSRC-TR-98-00158 (April, 1998).
2. D. C. Losey, "Decay Heat Characterization of SRS Research Reactor Fuels", WSMS-CRT-97-0016 (February, 1998).
3. *CFX-4.2: Environment*, AEA Technology, (1997).
4. S. Y. Lee, "Three-Dimensional Thermal Analysis and Simulation of Dry Spent Nuclear Fuel Storage Canister Using CFDS-FLOW3D (U)", WSRC-TR-96-0059 (March, 1996).
5. "Mined Geologic Disposal System Draft Disposability Interface Specification," B00000000-0171704600-00108 REV 00, February 1998, prepared for U. S. Department of Energy, Yucca Mountain Site Characterization Office, by TRW Environmental Safety Systems, Inc.
6. R. L. Sindelar, "Plan for Direct/Co-Disposal Technology Development and Form Assessment for DOE Aluminum-Based Spent Nuclear Fuel", SRT-MTS-97-2030, October 7, 1997.
7. D. Vinson, "Preliminary Material Property Data", e-mail message (September 5, 1997).
8. T. Adams, "Melt-Dilute Values", e-mail message, (February 6, 1998). Also see WSRC-RP-89-489 report.
9. A. J. Chapman, *Heat Transfer*, Third Edition, Macmillan Publishing Co., Inc., (1974).
10. J. Jerrell, S. Y. Lee, and A. Shadday, "Thermal Analysis of the Failed Equipment Storage Vault System (U)", WSRC-TR-95-0288, (1995).
11. Kays, W. M. and Crawford, M. E., *Convective Heat and Mass Transfer*, Second Edition, McGraw-Hill Book Company, (1980).
12. S. V. Patankar, *Numerical Heat Transfer and Fluid Flow*, Hemisphere Publishing Corporation, (1980).
13. R. L. Sindelar, "Alternative Aluminum Spent Nuclear Fuel Treatment Technology Development Status Report (U)", WSRC-TR-97-00345 (October, 1997).

Report: WSRC-TR-98-00299
Date: 05/10/99

WESTINGHOUSE SAVANNAH RIVER COMPANY

Page: 56 of 56

THERMAL ANALYSIS OF REPOSITORY CODISPOSAL WASTE
PACKAGES CONTAINING MELT-DILUTE ALUMINUM SPENT NUCLEAR FUEL

(This Page Intentionally Left Blank)

WESTINGHOUSE SAVANNAH RIVER CO. REPORT WSRC-TR-98-00299

DISTRIBUTION

SAVANNAH RIVER SITE

W. Poulson, 704-C
S. Wood, 773-A
G. T. Wright, 773-A
G. H. Clare, 704-C
M. W. Barlow, 704-C
E. R. Conatser, 704-C
M. E. Dupont, 707-C
R. J. Skwarek, 704-C
W. F. Swift, 707-C
H. M. Brooks, 704-C
W. S. Large, 707-C
G. Reynolds, 704-C
T. J. Worrell, 705-K
D. J. Green, 773-A
M. A. Ebra, 773-42A
C. P. Holding-Smith, 773-42A
C. R. Wolfe, 773-A
T. L. Capeletti, 773-41A
N. C. Iyer, 773-A
M. R. Louthan, Jr., 773-A
S. Y. Lee, 773-42A
H. B. Peacock, Jr., 773-A
T. M. Adams, 773-41A
A. J. Duncan, 773-41A

P. S. Lam, 773-41A
W. F. Ayres, 773-41A
D. W. Vinson, 773-41A
R. L. Sindelar, 773-41A
Site Records, 773-52A